Time Series Analysis of Fermi-LAT Blazars

A Dissertation

Submitted in Partial Fulfillment of the Requirement for the Award of

Degree of

Master of Science

In

Physics

Submitted By:

Pranjal Chaturvedi

Roll No. 302104005

Under the supervision of:

Dr. Raj Kumar
Associate Professor
TIET Patiala

Dr. Krishna Kumar Singh
Scientific Officer (F)
BARC Mumbai

SCHOOL OF PHYSICS AND MATERIALS SCIENCE

THAPAR INSTITUTE OF ENGINEERING AND TECHNOLOGY, PATIALA

PUNJAB-147004

JULY-2023

Dedicated to My Family,

And My Friends.

Declaration

I hereby declare that the dissertation entitled **"Time Series Analysis of Fermi-LAT Blazars"** is an authentic record of my work carried out as a requirement for the award of the degree of **Master of Science** at **Thapar Institute of Engineering and Technology, Patiala** under the supervision of **Dr. Raj Kumar**, Associate Professor, School of Physics and Materials Science, Thapar Institute of Engineering and Technology, Patiala and **Dr. Krishna Kumar Singh**, Scientific Officer (F), Astrophysical Sciences Division, Bhabha Atomic Research Center, Mumbai. No part of the matter embodied in this dissertation has been submitted to any other university or institute for the award of any degree.

Dated:31/07/2023

(Pranjal Chaturvedi)

3013204005

It is certified that the above statement made by the student is correct to the best of my knowledge and belief.

(Dr. Raj Kumar)
Associate Professor
TIET Patiala

(Dr. Krishna Kumar Singh)
Scientific Officer (F)
BARC Mumbai

Acknowledgment

With a heartfelt sense of gratitude, I wish to acknowledge the opportunity and valuable guidance rendered to me by **Dr Raj Kumar**, Associate Professor, Thapar Institute of Engineering and Technology and **Dr Krishna Kumar Singh**, Scientific Officer (F), Astrophysical Sciences Division, Bhabha Atomic Research Center. I am incredibly thankful to them for their humility in taking me as their student and believing in me to undertake the problem I was given during this work. I am thankful to **Dr Raj Kumar** and **Dr Krishna Kumar Singh** for giving me the flexibility and liberty to carry out this work.

I am highly obliged to **Dr Kulvir Singh**, Head of Department, School of Physics and Materials Science, Thapar Institute of Engineering and Technology and **Dr K K Yadav**, Head, Astrophysical Sciences Division, Bhabha Atomic Research Centre for their guidance during various stage of this work. I want to embrace this opportunity to acknowledge my gratitude towards all the faculty members of the School of Physics and Materials Science who were always accessible and helpful.

At last, I wish to sincerely thank my family, my friends, and my classmates for their support and all the scientists who devoted their entire life to the pursuit of truth and understanding of how nature behaves the way it does.

(Pranjal Chaturvedi)

Contents

List of Figures

List of Tables

Abstract

Active Galactic Nuclei (AGN) are extremely energetic sources with an intense luminescence emanating from the center of galaxies, caused by matter accretion on the SMBH. These luminous objects are essential for measuring cosmological distances and epochs, but their study is expanding swiftly in astrophysics due to the high rates and small scales at which they release energy. AGNs are divided into two primary categories: radio-loud and radio-quiet.

Researchers have searched for Quasi Periodic Oscillations (QPOs) in AGNs for years, but the Fermi-LAT has provided ample data for long-term studies. Some studies have observed QPOs in gamma wavelength, with jets being the primary emission source. The binary black hole model is better explained for decade-long periodicities, while jets are better explained for year-time periodicities. Multiple physical models have been formulated to explain the existence of QPOs in AGNs. Variability in the AGNs are typically divided into three time scales, Intra Day Variability (IDV), Short Term Variability (STV), Long Term Variability (LTV). IDV spans on the timescale of a few minutes to less than a day, STV spans the timescale of a day to a few weeks or months and LTV spans over a few months to years.

The search for QPOs in gamma-ray Light Curve (LC) involves treating the Light Curve as a time series and applying time series analysis methods. Common methods include Lomb Scargle Periodogram (LSP), Weighted Wavelet Z Transform (WWZT), and Power Spectral Density (PSD). In this study, LSP and WWZT are used simultaneously to search for QPOs. LSP is a version of the Discrete Fourier Transform (DFT) and is used to find periodicities in unevenly spaced temporal signals. WWZT, on the other hand, is a widely used wavelet transform method that fits sinusoidal signals varying frequency and location in the time series, allowing for identifying QPOs in specific parts of the time series.

Multiple nations have collaborated on the Fermi Gamma-ray Space Telescope to investigate the universe at Gamma wavelength. In 1991, the Energetic Gamma Ray Experiment Telescope (EGRET) conducted the first comprehensive sky survey in the high High Energy Gamma Ray wavelength. Fermi features two instruments: an enhanced version of the gamma-ray imaging spectrometer onboard EGRET and another instrument to investigate gamma-ray bursts (GRB). The primary instrument, the Large Area Telescope

(LAT), has a higher sensitivity, allowing for a more comprehensive coverage of transient phenomena. The Gamma Burst Monitor (GBM) is a secondary instrument designed to observe GRBs.

This study has shown that there is a very good possibility of QPOs in gamma wavelength that were previously not noticed due to a lack of long-term data. Further, it is shown in the study that the QPO observed has no correlation between the Mass of SMBH at the centre of the galaxy and observed periodicity. Similarly, no correlation was observed between the Redshift of the galaxy and observed periodicity.

Chapter 1

Introduction

1.1 Active Galactic Nuclei (AGN)

Active Galactic Nuclei (AGN) are highly energetic sources characterised by an exceptionally bright glow from the galaxy's centre. They are powered by the accretion of matter on the SMBH in the galaxies. The emission is observed in the whole electromagnetic spectra, and the emission goes up to TeV energy levels[19]. The study of active galactic nuclei is a rapidly growing area in astrophysics, as they are the sites of energy release at powerful rates and compact scales. These luminous objects serve as markers of the distant reaches of the universe. Understanding their physical nature and structure is crucial for measuring cosmological distances and times. However, reviewing this field is challenging due to the vast number of papers covering various research methods[18].
AGNs are characterised in two major categories, Radio Loud AGNs and Radio Quiet AGNs.
Radio Loud AGNs are divided into these classes:

- Quasars: Quasars or Quasi-Stellar Objects (QSOs) can be classified in both groups, as some quasars have been observed to emit radio waves. Additionally, a few did not transmit radio wavelength. They are the brightest AGNs and have a spectrum similar to Seyfert's. In contrast, their stellar absorption features are either feeble or absent, indicating that they are likely less dense in terms of gas, and their emission lines are narrower and weaker than Seyfert's.

- Blazars – Blazars are characterised by their rapidly varying emission, with their luminosity changing by up to 50% daily. Emission line features are intrinsically absent in blazars. These are further divided into two subclasses, BL Lacertae and Optically Violent Variable Quasars.

- Radio Galaxies: As implied by their classification, radio galaxies are potent emitters of radio emission. These are elliptical galaxies with nuclear radio emission, typically accompanied by single or twin radio lobes (spanning the galaxy) that can be on the order of Mpc in size. Narrow radio jets occasionally connect radio lobes and nuclear radio emissions.

Radio quiet AGNs are further divided into these classes:

- Seyfert Galaxies: Carl Seyfert discovered the initial classification of AGNs. These were later divided into Type 1 and Type 2 subclasses. In Type 1 Seyfert galaxies, both broad and narrow emission lines are visible, whereas only broad emission lines are visible in Type 2 Seyfert galaxies.

- Low Ionisation Nuclear Emission-Line Region (LINERs): LINERs show weak nuclear emission lines. They do not show any other signature AGN emission. These have the lowest luminosity among all AGNs, and whether their emission is even through the accretion disc is a subject of study.

1.1.1 Blazars

Blazars are AGN objects with their relativistic jets pointed towards the Earth. The jets originate in the central part of the galaxy and typically extend upto scale of Mpc. The jets are believed to originate in the central region of the galaxy. The bolometric luminosity measured from the blazar indicates a high accretion rate on to the center of the galaxy. It is the consensus that the jets are powered by the spinning of the SMBH at the center of the galaxy. Over Mpc scales, the relativistic jets convey a large quantity of momentum and energy, and lose only a minor amount of energy during their trajectory. The content of the jets and the physical processes responsible for the jet have not yet been identified. Blazars have been observed to emit in wavelengths encompassing Radio to TeV radiation due to nonthermal emissions from the jet. The blazars are divided into BL Lacertae (BL Lac) and Flat Spectrum Radio Quasar (FSRQ) objects. The FSRQ objects exhibit little to no variability in the Radio wavelength, whereas BL Lac objects exhibit variability in all wavelengths[25].

1.2 Quasi Periodic Oscillations (QPO)

Researchers have long sought after QPOs in AGNs, observing in all wavelengths. Search for QPOs is a relatively new field of study, mainly due to a lack of long-term data. But now, Fermi-LAT has been collecting data for around one and a half decades, providing ample data for long-term studies. A few studies have observed QPOs in AGNs in gamma wavelength [9, 14, 24, 26, 31, 32]. Since the majority of emission in gamma wavelength

originates in the jets, the cause of periodicity must lie in the jet. In the case of decade-long periodicities, they are better explained by the binary black hole model [24]. In contrast, the periodicities on year timescales are better explained by jets.
Multiple physical models have been formulated to explain the existence of QPOs in AGNs. Some of the recent theories are listed below.

1.2.1 Bending of Relativistic Jet/Inhomogeneous Jet

The Doppler factor is influenced by the bulk Lorentz factor (Γ) and the observing angle. Variations in Γ along the jet and in time are conceivable, but would necessitate substantial differential accelerations or decelerations of the bulk flow. Rather, orientation changes induce Doppler factor variations, which is the premise. Non-axisymmetric instabilities in magnetohydrodynamic jet simulations and observations of CTA 10224 and blazars with whirling jets or helical jet structures provide support for this theory. The viewing angle can be derived as a function of time using $\delta(t)$ and an estimate for Γ. When the emitting region becomes better aligned with the line of sight, the flux increases at a particular frequency. If all emitting regions had the same orientation, the residual variability would correspond to rapid outbursts, which are most likely the result of intrinsic energetic processes. Compared to the original factor of 600, the dispersion factor during the various observing seasons has been decreased to 2 (0.009-0.022 mJy). This indicates that emission at different frequencies originates from distinct regions along a continuous jet with varying orientations with respect to the line of sight over time. [21].

1.2.2 Precession of the Jet Due to Interaction in a Binary SMBH system

The observed periodicities may arise due to a periodically varying viewing angle which is driven by orbital motion, precessing jet, or an internally rotating jet flow. The expected period is < 10 days, even for the massive quasars and objects with large bulk factors [10]. (Lu, 2005)[16] predicted the precession period of a jet for a single SMBH as

$$\log(\tau_{\rm prec}/{\rm yr}) \sim 0.48 M_{\rm abs} + 0.14 \log\left(\frac{M}{10^8\,{\rm M}_\odot}\right) + A \tag{1.1}$$

where A = 15.18-18.86, Mabs is the absolute magnitude, and M is the mass of BH in M_{odot}. For a typical Quasar with Mabs = -25 and M = $10^8 M_{odot}$, the period comes out to be between 102.2 and 106.9 years. This period is much longer than observed in any study yet. Following this formula, a binary SMBH system may exhibit shorter time periods for jet precession.

1.2.3 Warped Accretion Disk in Binary SMBH

Nuclear discs may get warped after going through multiple processes. When the planar disc is inclined perpendicularly to the spin of the host black hole, it starts precessing due to the Bardeen effect [7]. Another process is when the disc's angular momentum is aligned with the angular momentum of the black hole due to torque arising from the internal viscosity. The timescale of this alignment is close to the Eddington limit, i.e. ($t \leq 10^6 yrs$) for an SMBH of mass $10^8 M_\odot$. Observations from NGC 4258 and NGC 1068 fit the effect satisfactorily well, as the radius of alignment was well within the limits of observed maser spots. The warped disc is not uniformly illuminated when exposed to light from the structure's interior. The radiation absorbed by an optically opaque disk is re-emitted perpendicularly with respect to the disk plane near the point of emission. This emission produces torque in the disk and warps it. Planar disks may warp if their radius $r \leq 0.1pc$ and vertical and radial viscosity coefficients are similar. Warps due to gravitational effects have been studied mainly on the galactic level [29].

There are many other models developed over the years, covering all the parts of the AGN, the torus, the Broad Line Region clouds, the Narrow Line Region clouds and the jet. The models described above describe the possible options that could cause QPOs in AGNs.

1.3 Fermi-LAT Data and Analysis

The Fermi Gamma-ray Space Telescope is a collaborative effort between multiple countries to study the universe in Gamma wavelength. The first complete sky survey in the

high High Energy Gamma Ray wavelength was conducted by Energetic Gamma Ray Experiment Telescope (EGRET) in 1991. The survey intrigued the researchers as it divulged the turbulent nature of the sky in Gamma Ray wavelength. Fermi hosts two instruments, an improved version of the gamma-ray imaging telescope onboard the EGRET and another instrument to study gamma-ray bursts (GRB). The primary instrument, the Large Area Telescope (LAT), has better sensitivity, providing better coverage of the transient phenomena. The secondary instrument, the Gamma Burst Monitor (GBM), is dedicated to observing GRBs.[4].

High-energy gamma rays are detected using technology similar to detectors in particle accelerators. Incident gamma rays fall on the anti-coincidence detector to eliminate the background radiation. The incident cosmic rays produce a flash of light which is ignored. The LAT identifies rare gamma rays, which interact with atoms, producing electrons and positrons. They create ions in thin silicon strip detectors, which track their progress in X and Y directions. The information from a Caesium Iodide Calorimeter provides an estimate of the directon and energy of incident gamma ray[2].

The Fermi LAT data is available on the Light Curve Repository website [3]. The data on the website is processed and available for download in multiple binning options, 3 days, 7 days, and 30 days. The LCR analysis uses Fermi LAT science tools and $P8R2\_SOURCE\_V6$ instrument response functions on $P8R3\_SOURCE$ class photons over 100 MeV-100 GeV energy range. Data selection includes a 12° radius ROI, extra data selection cuts to exclude solar flare and GRB activity, and a 90° zenith angle cut to prevent contamination from cosmic rays. The data model models the counts distribution for each source of interest as a point source using an energy-dependent LAT PSF and a photon spectrum from the 4FGL-DR2catalogue. The normalisation of the source spectrum can vary, catalogue values are taken as default values for spectral values. The data takes into account all the gamma ray sources in a 30° radius and the galactic and isotropic background noise is normalised. To increase the probability of observing data, the free parameters are adjusted. To reduce the number of bins with weak likelihood fits, an iterative fitting method is used. After obtaining a good fit, a second round of fitting is carried out using a variable photon index for the source of interest.[1].

Chapter 2

Methodology

2.1 Methodology

The idea behind looking for a QPO is to treat the Light Curve as a time series and apply time series analysis methods to the LC. The most common methods for finding QPOs in gamma-ray LCs are Lomb Scargle Periodogram (LSP), Weighted Wavelet Z Transform (WWZT), Power Spectral Density (PSD) etc. In this study, LSP and WWZT are used simultaneously to search for QPOs.

2.1.1 Lomb Scargle Periodogram (LSP)

LSP is a version of the Discrete Fourier Transform (DFT), which was developed by Lomb, 1976 [15] and Scargle, 1982 [22]. It is a well-known method of finding periodicities in unevenly spaced temporal signals, especially in the astronomy community, where the data is often unevenly spaced, with large chunks missing. This method has multiple options like the Fourier Transform, Phase-folding, Least-Square, and Bayesian approaches.
Fourier methods are formed by combining the principles of Fourier. Transform and Power Spectra with Correlation Function Examples include the Schuster periodogram, the Lomb-Scargle periodogram, and the correlation-based method. Phase-folding methods involve folding observations as a function of phase, computing a cost function across the phased data, and optimising this cost function across candidate frequencies. Examples include String Length and Analysis of Variance (ANOVA). Least-squares methods comprise superimposing different functions with varying frequencies on the data, computing the goodness of fit for each frequency, and selecting the frequency that best fits. Examples include the Lomb–Scargle periodogram and orthogonal polynomial fits. Bayesian Approaches utilise the principles of Bayesian Probability to the data. The process can seem quite similar to phase folding and least-square methods. The Lomb–Scargle periodogram is a unique niche in the field, motivated by Fourier analysis but also derived from Bayesian probability theory principles and bin-based phase-folding techniques. Thus, the Lomb–Scargle periodogram creates a unique combination point of all the important methods of time series analysis[30].
This study calculates the LSP using the LombScargle() function in Python's AstroPy library[5].

2.1.2 Weighted Wavelet Z-Transform (WWZT)

The wavelet transform methods have been widely used in recent studies. The idea behind this method is to fit sinusoidal signals varying the frequency and the location of the sinusoidal signal in the time series. This gives the advantage of looking for QPOs that may exist only in a part of the time series and not overall [6]. Weighted Wavelet Z-Transform uses a Morlet Kernel [11] written as:

$$f[\omega(t-\tau)] = exp[i\omega(t-\tau) - c\omega^2(t-\tau)^2] \tag{2.1}$$

Furthermore, the WWZ map is given by:

$$W[\omega, \tau; x(t)] = \omega^{1/2} \int x(t) f^*[\omega(t-\tau)]dt \tag{2.2}$$

Where f^* is the complex conjugate of Morlet Kernel, c is the decay parameter, ω is the frequency, and τ is the time shift. The decay parameter determines how rapidly the kernel would decay; the higher the value faster the wavelet would decay. For variable light curves, the typical value of the decay parameter is $1/8\pi^2$.
The code for WWZT in this study is adapted from Templeton,2004[28].

2.2 Sources

The sources have been selected on the three conditions

- Data available from 1st Fermi catalogue till 4th Fermi catalogue
- Declination between +0° and +75°
- Redshift less than 1.25

The sources selected are as follows:

NAME	4FGL NAME	RA	DEC	Redshift	Mass ($M_\odot * 10^8$)
S2 0109+22	4FGL J0112.1+2245	01h 12m 05.82s	+22° 44" 38.79'	0.265	22 (1)
3C 66A	4FGL J0222.6+4302	02h 22m 39.61s	+43° 02" 07.79'	0.444	3.70 (2)
TXS 0518+211	4FGL J0521.7+2112	05h 21m 45.96s	+21° 12" 42.11'	0.108	6.31 (3)
S5 0716+714	4FGL J0721.9+7120	07h 21m 53.44s	+71° 20 36.34	0.127	11.0 (4)
1ES 0806+524	4FGL J0809.8+5218	08h 09m 49.18s	+52° 18" 58.24'	0.138	5.00 (5)
1H 1013+498	4FGL J1015.0+4926	10h 15m 04.13s	+49° 26" 00.7'	0.212	
PG 1218+304	4FGL J1221.3+3010	12h 21m 21.94s	+30° 10" 37.16'	0.182	2.80 (6)
PKS 1424+240	4FGL J1427.0+2348	14h 27m 00.39s	+23° 48" 00.03'	0.6	
Mkn 501	4FGL J1653.8+3945	16h 53m 52.21s	+39° 45" 36.61'	0.0337	21.5 (7)
BL Lac	4FGL J2202.7+4216	22h 02m 43.29s	+42° 16" 39.97'	0.0686	6.61 (8)

Table 2.1: BL Lacertae Sources. (1): Gong et al. (2022)[9], (2): Kaur et al. (2017)[12], (3): Shaw et al. (2013)[23], (4): Chandra et al. (2011)[8], (5): Osmanov (2010)[17], (6): Sun et al. (2021)[27], (7): Kranich et al. (1999)[13], (8): Paliya et al. (2021)[20]

NAME	4FGL NAME	RA	DEC	Redshift	Mass ($M_\odot * 10^8$)
TXS 0059+581	4FGL J0102.8+5824	01h 02m 45.76s	+58° 24" 11.12'	0.644	10.2 (1)
4C +28.07	4FGL J0237.8+2848	02h 37m 52.40s	+28° 48" 08.99'	1.213	13.4 (1)
B2 0716+33	4FGL J0719.3+3307	0)7h 19m 19.42s	+33°07" 09.69'	0.779	7.76 (1)
4C +71.07	4FGL J0841.3+7053	08h 41m 24.36s	+70° 53" 42.17'	2.218	158 (1)
S5 1044+71	4FGL J1048.4+7143	10h 48m 27.61s	+71° 43" 35.94'	1.15	14.4 (1)
3C 273	4FGL J1229.0+0202	12h 29m 06.70s	+02° 03" 08.6'	0.158	48.9 (1)
PKS 1441+25	4FGL J1443.9+2501	14h 43m 56.89s	+25° 01" 44.5'	0.939	1.02 (1)
TXS 1700+685	4FGL J1700.0+6830	17h 00m 09.29s	+68° 30" 06.94'	0.301	0.199 (1)
OX 169	4FGL J2143.5+1743	21h 43m 35.54s	+17° 43" 48.79'	0.213	10.2 (1)
3C 454.3	4FGL J2253.9+1609	22h 53m 57.74s	+16° 08" 53.55'	0.859	8.91 (1)

Table 2.2: Flat Spectrum Radio Quasar Sources. (1): Paliya et al. (2021)[20]

Chapter 3

Results and Conclusions

3.1 Results

This section presents results from time series analysis for the selected sources. The QPO and redshift of the sources are compared. QPO and mass are also compared in this section, and the implications of these results are discussed in detail. Most of the QPOs found in the sources were not mentioned in the literature. The found and QPO in the literature were close for a few sources, with a maximum error of around 15%. The QPOs were found with False Alarm Probability (FAP) $\leq 5\%$.

NAME	4FGL NAME	Frequency ($Days^{-1} * 10^{-4}$)	Periodicity ($Year$)
3C 66A	4FGL J0222.6+4302	3.45	7.94
1ES 0806+524	4FGL J0809.8+5218	7.17	3.82
1H 1013+498	4FGL J1015.0+4926	1.40	19.57
PG 1218+304	4FGL J1221.3+3010	3.26	8.40
PKS 1424+240	4FGL J1427.0+2348	8.38	3.27
Mkn 501	4FGL J1653.8+3945	2.89	9.48
BL Lac	4FGL J2202.7+4216	5.50	4.98

Table 3.1: New QPOs in BL Lacertae Sources.

NAME	4FGL NAME	Frequency ($Days^{-1} * 10^{-4}$)	Periodicity $Year$	QPO in Literature ($Year$)	Error (%)
S2 0109+22	4FGL J0112.1+2245	9.78	2.80	2.45[9]	12.5
TXS 0518+211	4FGL J0521.7+2112	8.84	3.10	2.6[32]	16.1
S5 0716+714	4FGL J0721.9+7120	9.50	2.88	2.63[14]	8.7

Table 3.2: QPOs mentioned in literature for BL Lacertae Sources.

The periodicity of approximately 19.6 years in 1H 1013+498 strongly indicates the presence of a binary SMBH system at the core of the blazar as in the case of OJ 287 [24]. While in the other sources, the periodicities are of a timescale of a few years and cannot be attributed to a single process with confirmation.

Similarly, in FSRQ sources, the timescale of periodicity of all sources is of the order of a few years. The tables 3.3 and 3.4 give the exact details.

NAME	4FGL NAME	Frequency ($Days^{-1} * 10^{-4}$)	Periodicity ($Year$)
TXS 0059+581	4FGL J0102.8+5824	6.42	4.27
4C +28.07	4FGL J0237.8+2848	4.19	6.54
B2 0716+33	4FGL J0719.3+3307	1.58	17.34
4C +71.07	4FGL J0841.3+7053	2.51	10.92
3C 273	4FGL J1229.0+0202	4.57	6.00
PKS 1441+25	4FGL J1443.9+2501	2.90	9.45
OX 169	4FGL J2143.5+1743	1.24	22.09
3C 454.3	4FGL J2253.9+1609	3.26	8.40

Table 3.3: New QPOs in Flat Spectrum Radio Quasar Sources.

NAME	4FGL NAME	Frequency ($Days^{-1} * 10^{-4}$)	Periodicity ($Year$)	QPO in Literature ($Year$)	Error (%)
S5 1044+71	4FGL J1048.4+7143	8.89	3.08	3.06[31]	0.65

Table 3.4: QPOs mentioned in literature for Flat Spectrum Radio Quasar Sources.

Similarly, for OX 169, periodicity can confirm a presence of a supermassive binary, as proposed by [26] in their 1991 paper.

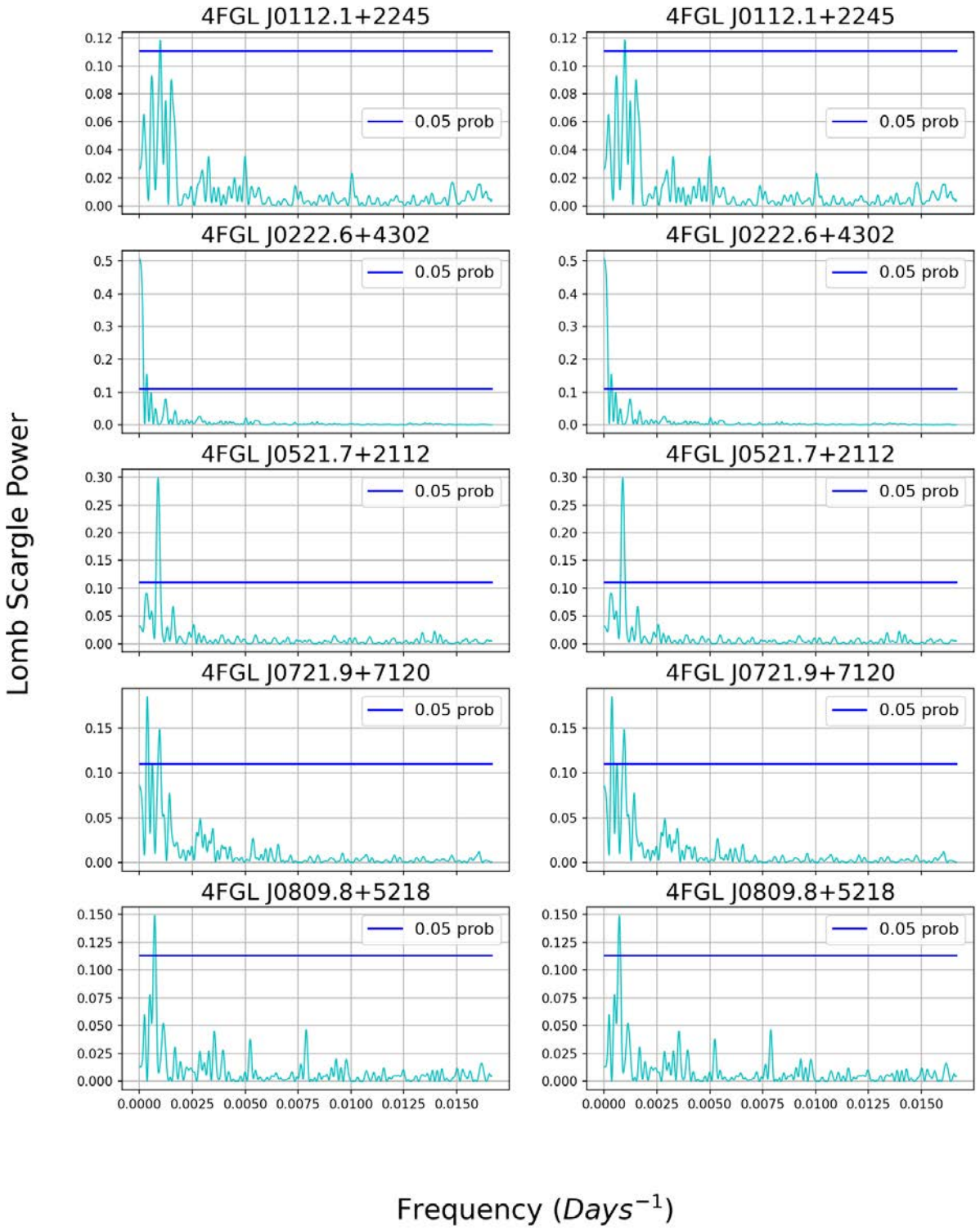

Figure 3.1: Lomb Scargle Periodogram of BL Lac sources. The dark blue line shows 5% False Alarm Probability (FAP), any point above this line has $FAP \leq 5\%$.

The Fig 3.1 shows that the sources have peaks at low frequencies; the LSP was limited to low frequencies to understand the peaks further.

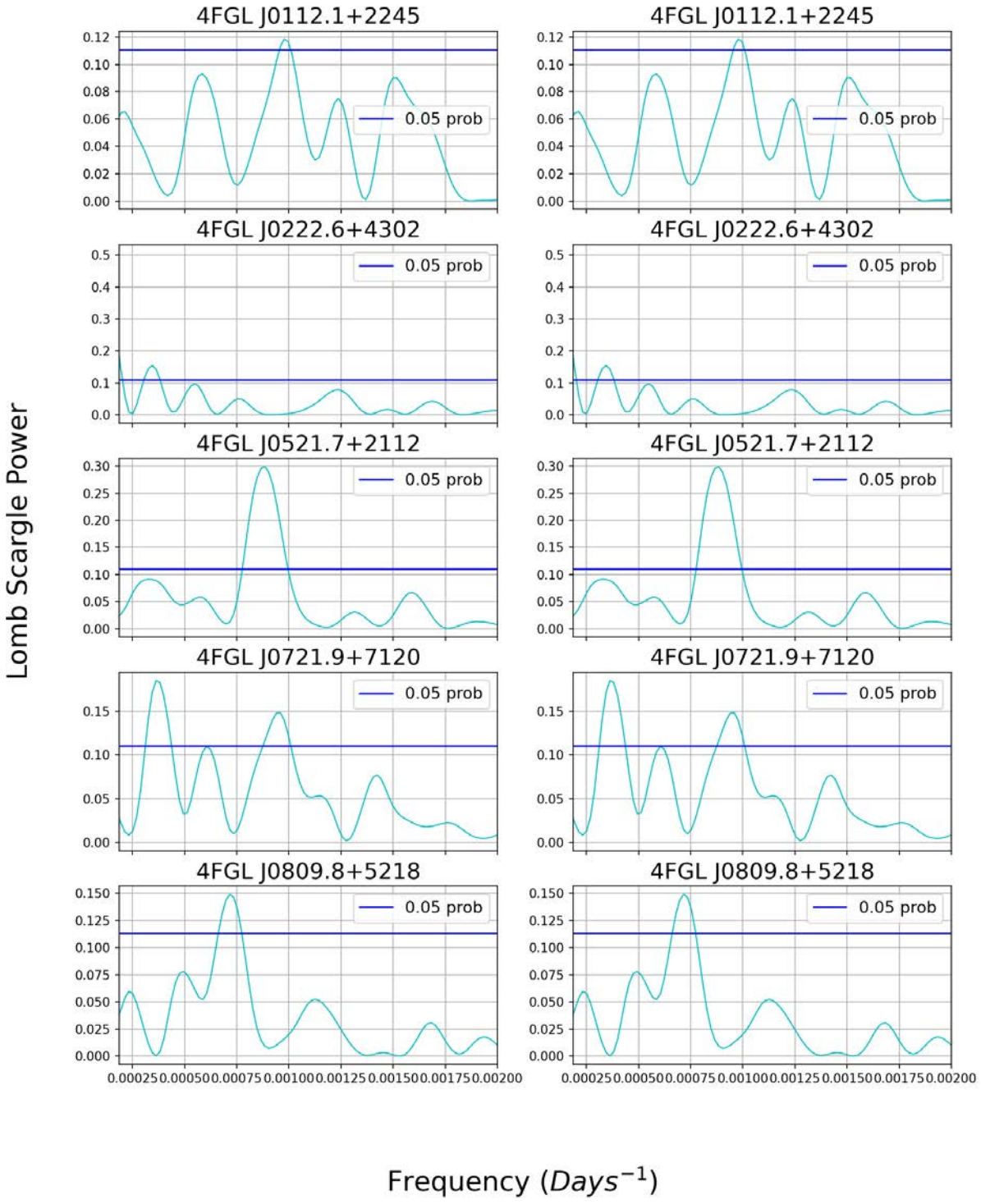

Figure 3.2: Zoomed in LSP of BL Lac sources.

The Weighted Wavelet Z-Transform (WWZT) of the light curve was taken to confirm these peaks. The WWZT peaks match LSP and thus confirm that the peaks were not false.

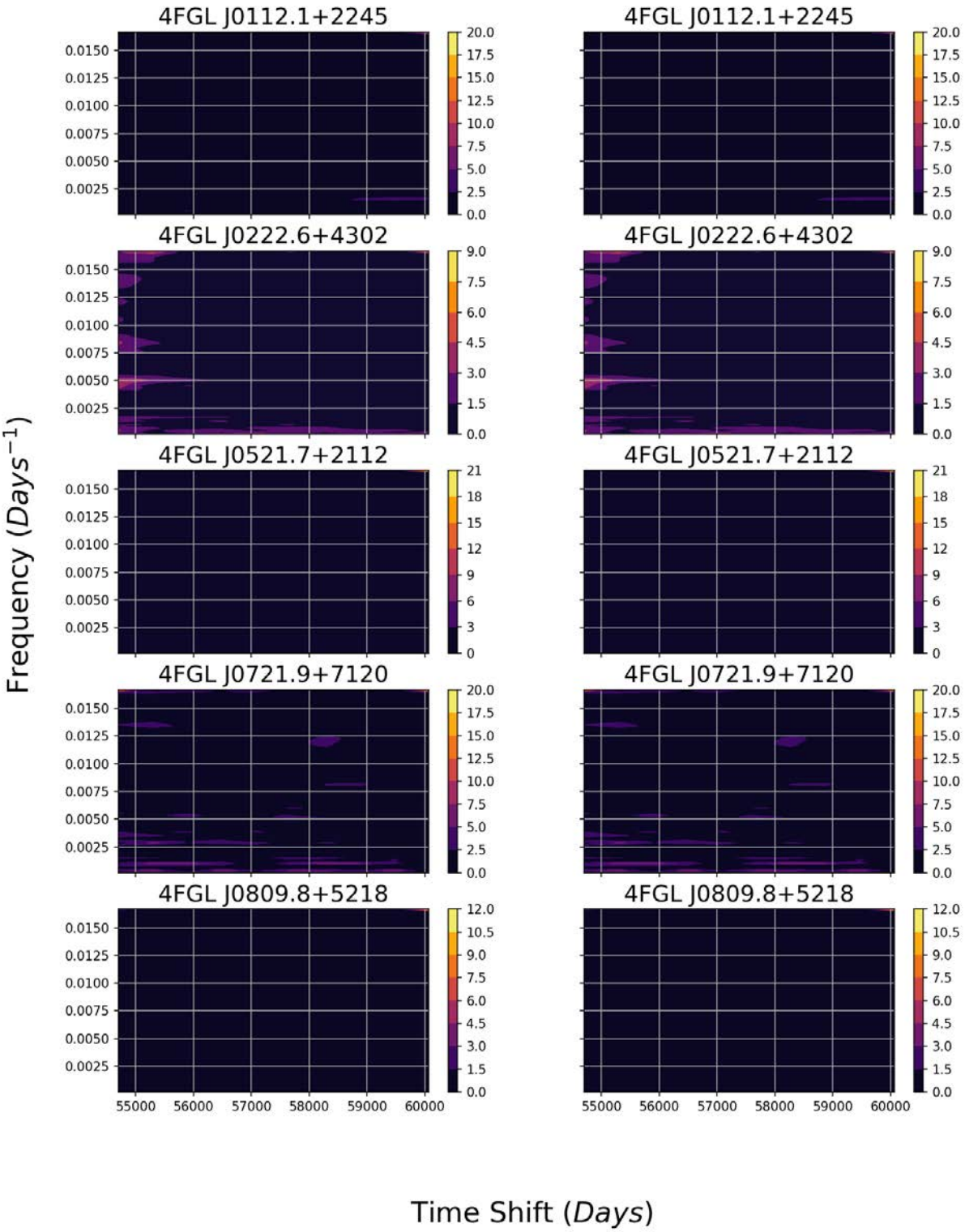

Figure 3.3: WWZT of BL Lac Sources. The power has a multiplication factor of 10^{-8}.

The WWZT diagrams were also further limited to low frequencies to show the peaks clearly.

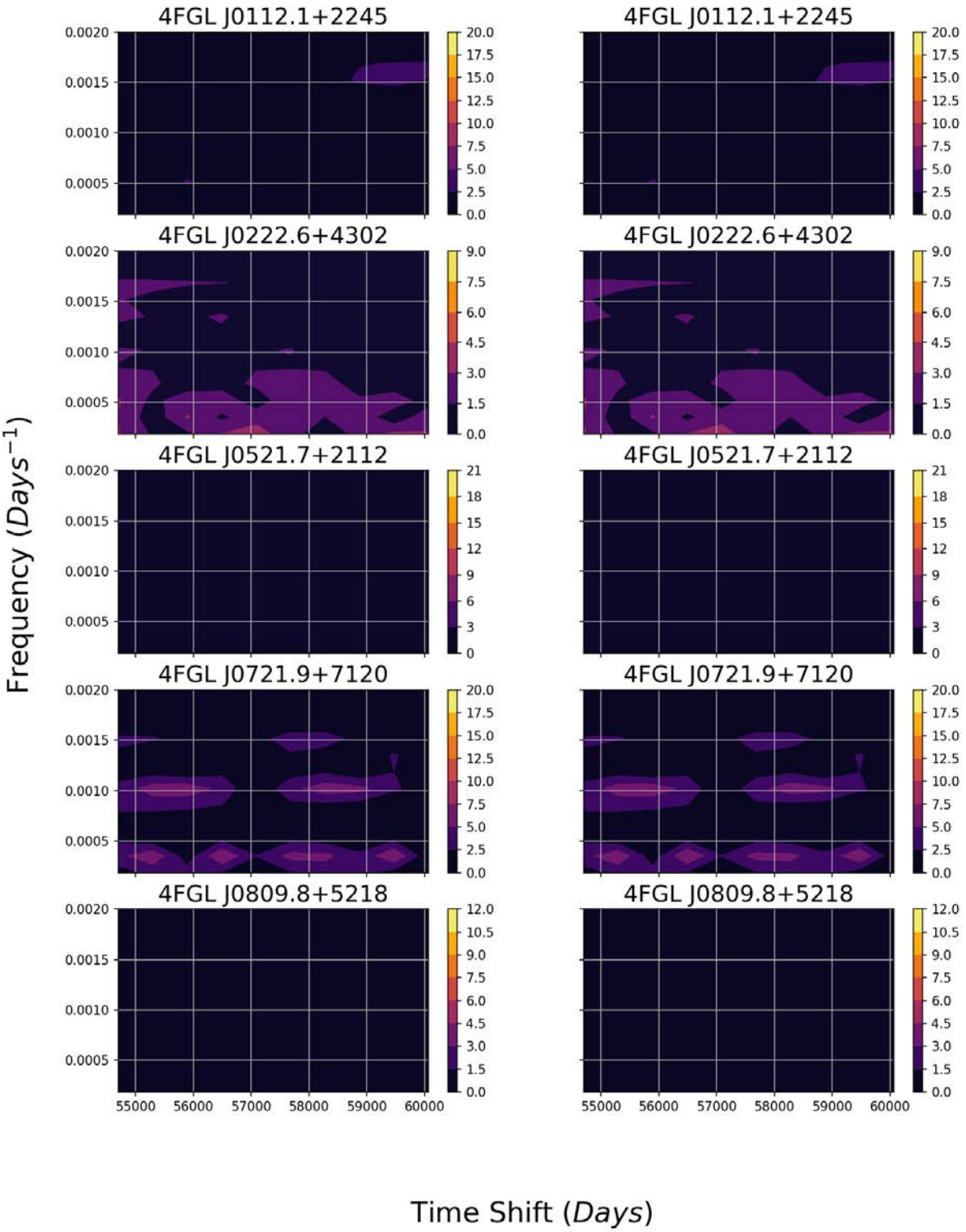

Figure 3.4: Zoomed in WWZT of BL Lac sources. The power has a multiplication factor of 10^{-8}.

The exact process was done for FSRQ objects, and similar results were obtained.

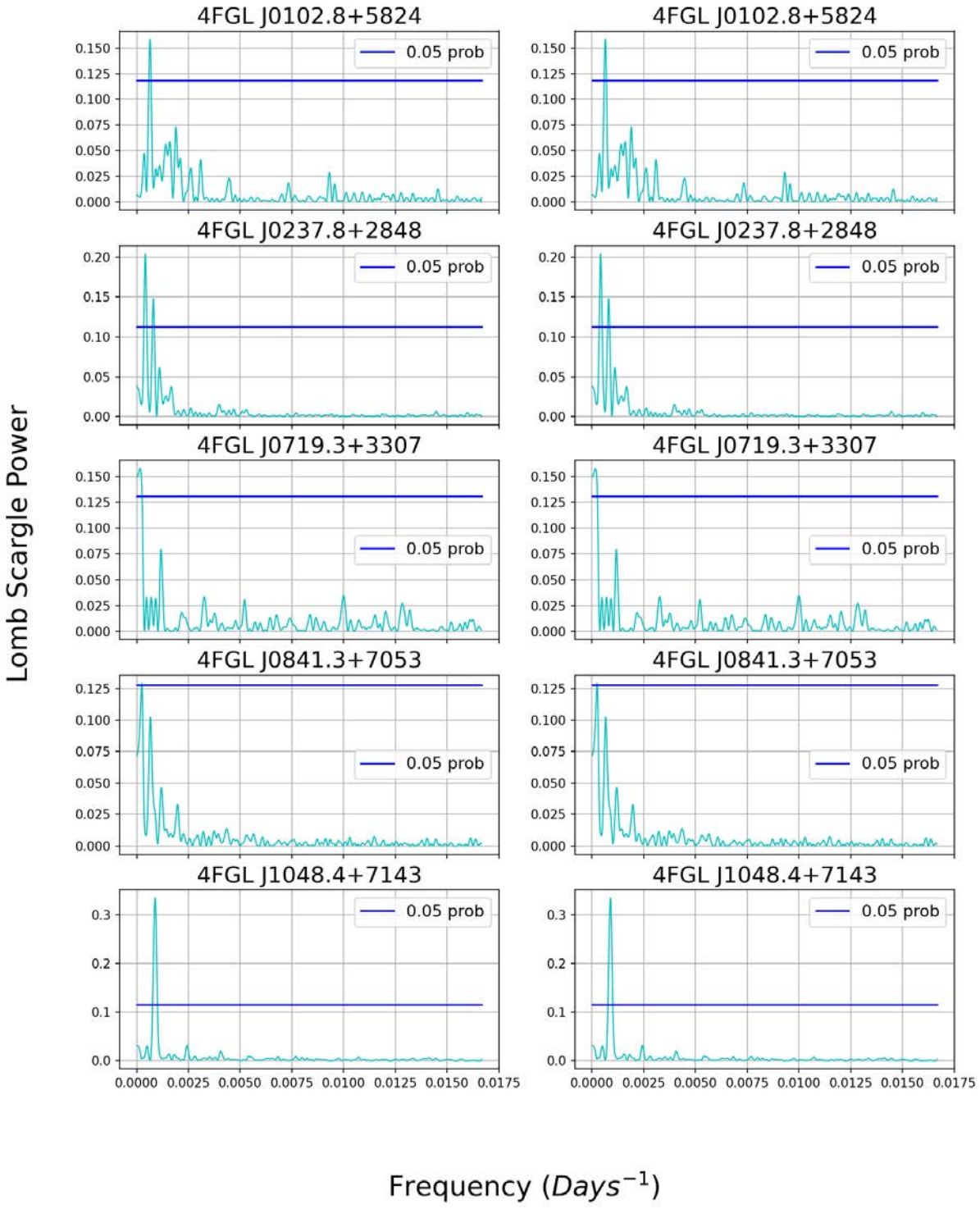

Figure 3.5: Lomb Scargle Periodogram of FSRQ sources. The dark blue line shows 5% False Alarm Probability (FAP), any point above this line has $FAP \leq 5\%$.

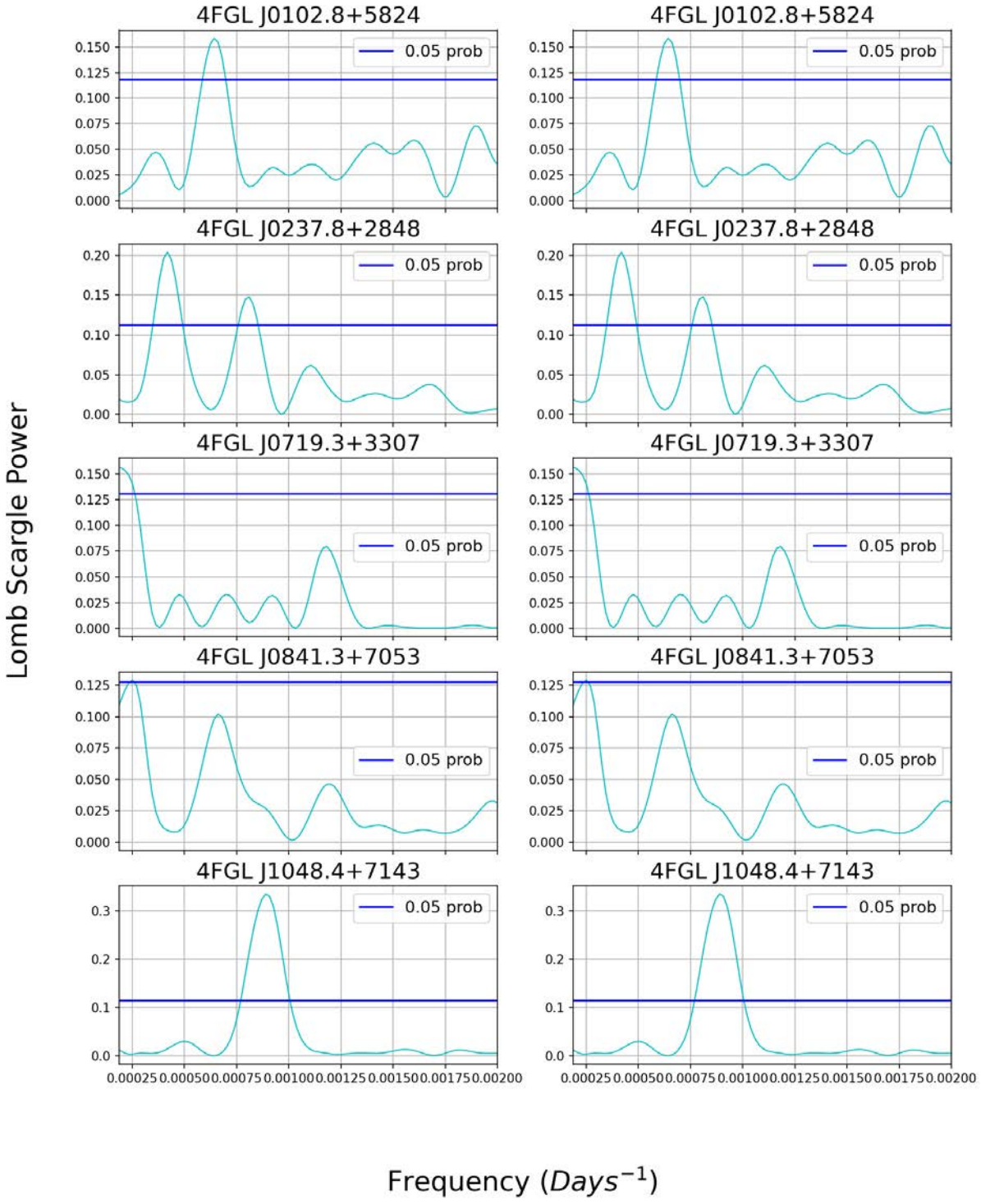

Figure 3.6: Zoomed in LSP of FSRQ sources.

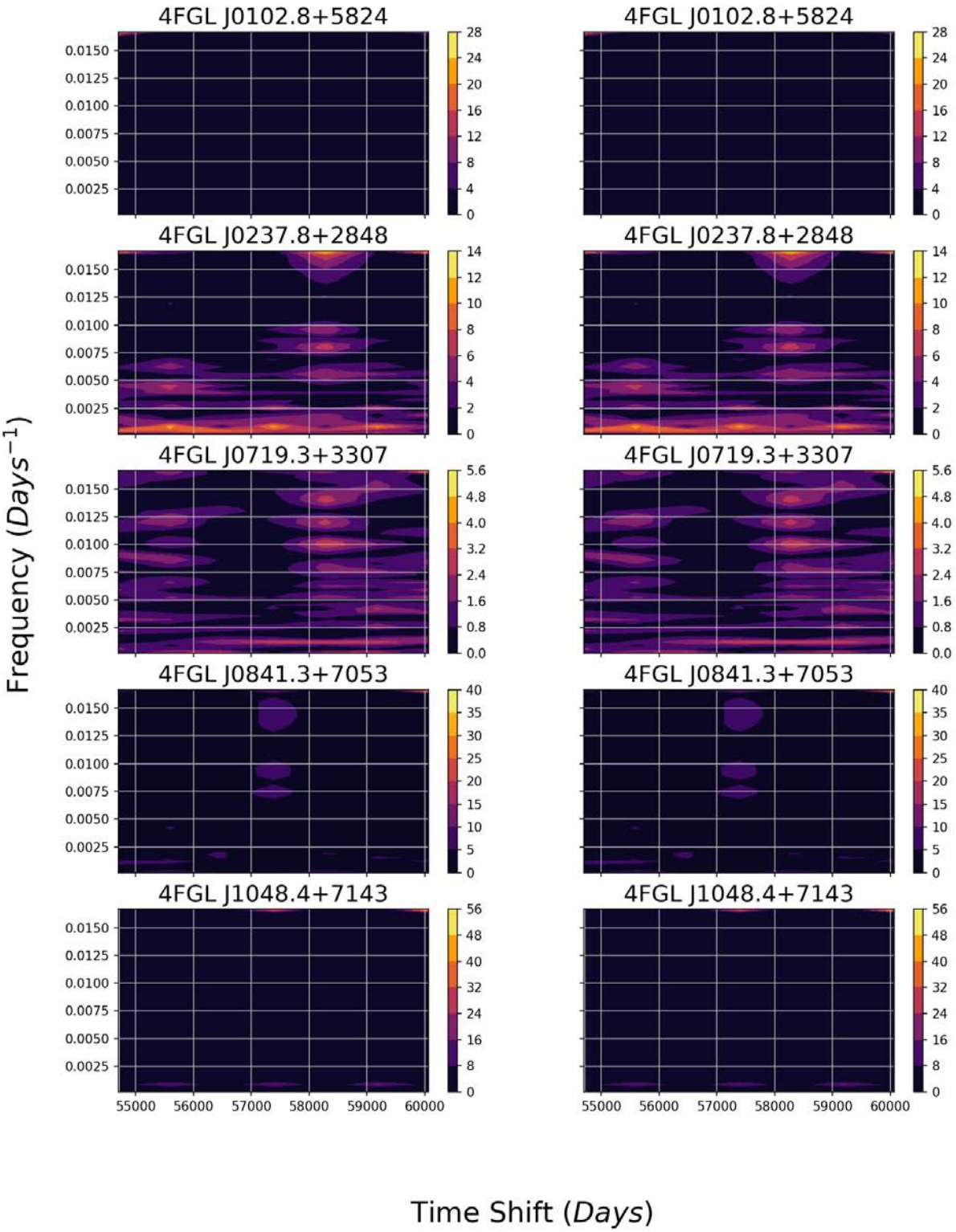

Figure 3.7: WWZT of FSRQ Sources. The power has a multiplication factor of 10^{-8}.

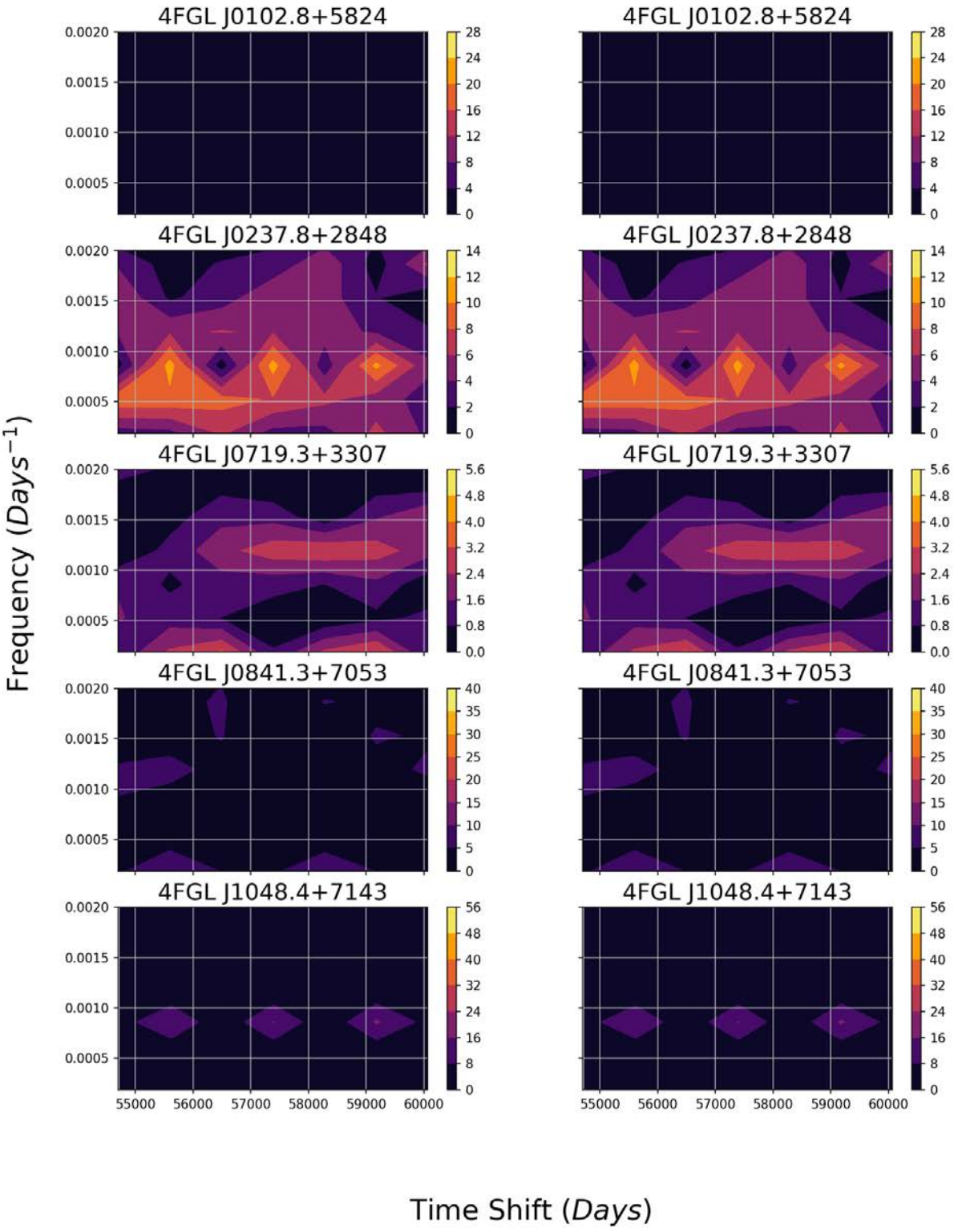

Figure 3.8: Zoomed in WWZT of FSRQ sources. The power has a multiplication factor of 10^{-8}.

After generating these diagrams, the found periodicity corresponded with the light curves shown below Figures 3.9 to 3.27. In the Figures, the orange curves represent the fitted sinusoidal function and blue dots represent the light curve.

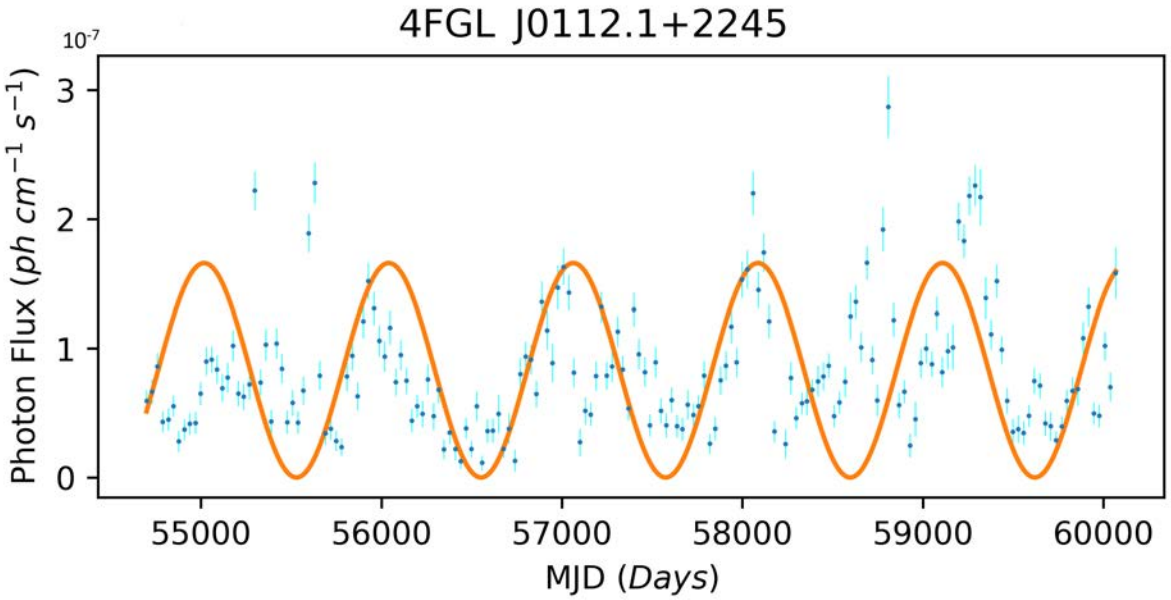

Figure 3.9: Sinusoidal curve fitted to light curve of S2 0109+22.

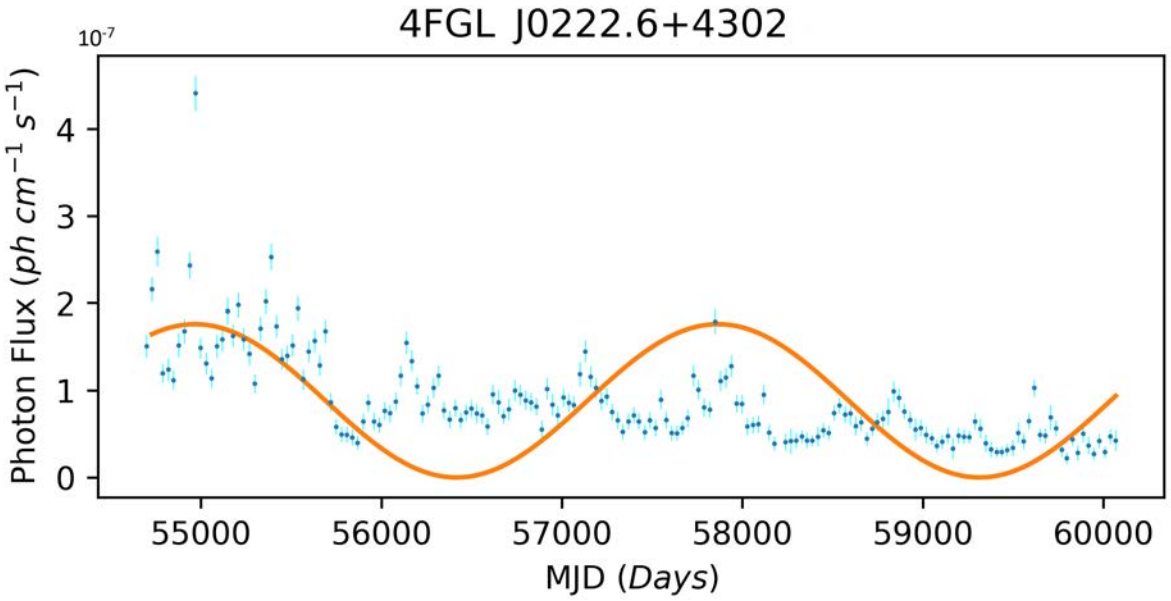

Figure 3.10: Sinusoidal curve fitted to light curve of 3C 66A.

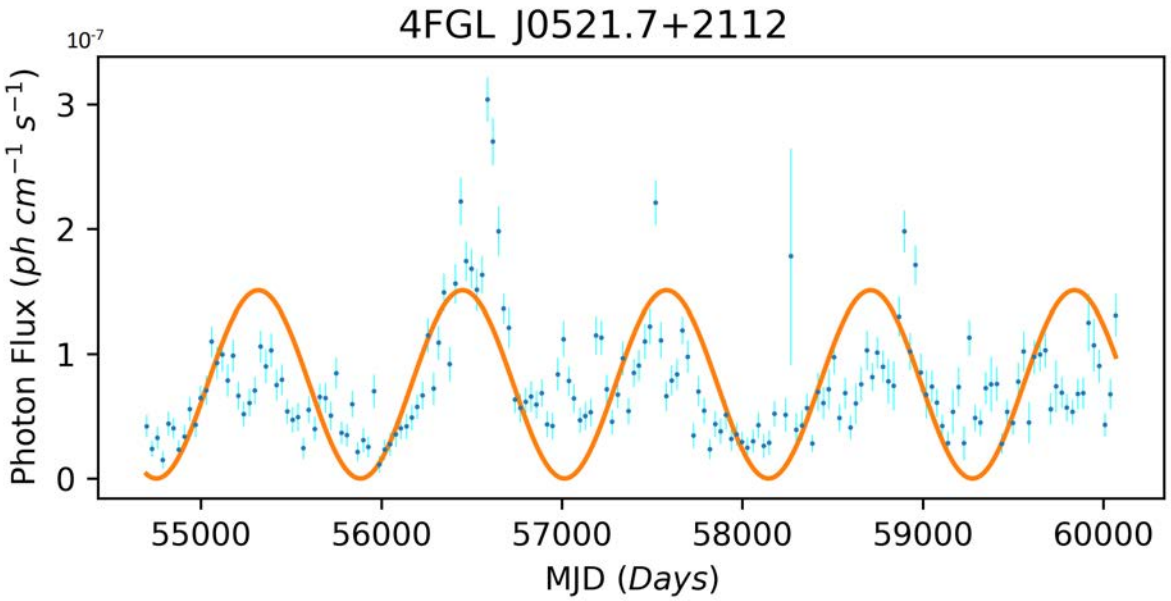

Figure 3.11: Sinusoidal curve fitted to light curve of TXS 0518+211.

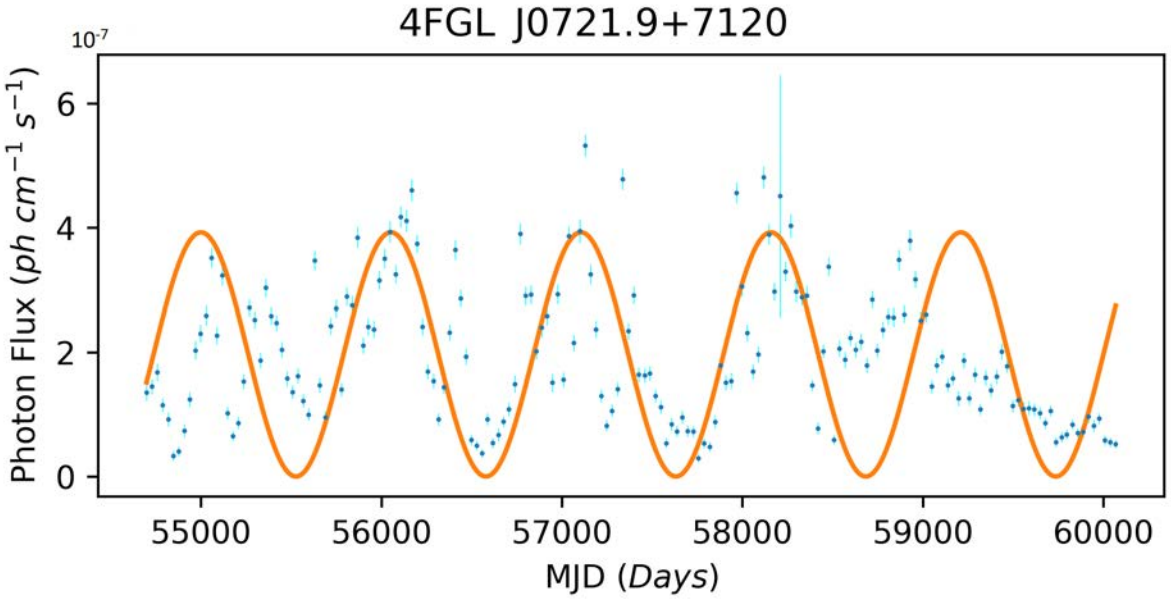

Figure 3.12: Sinusoidal curve fitted to light curve of S5 0716+714.

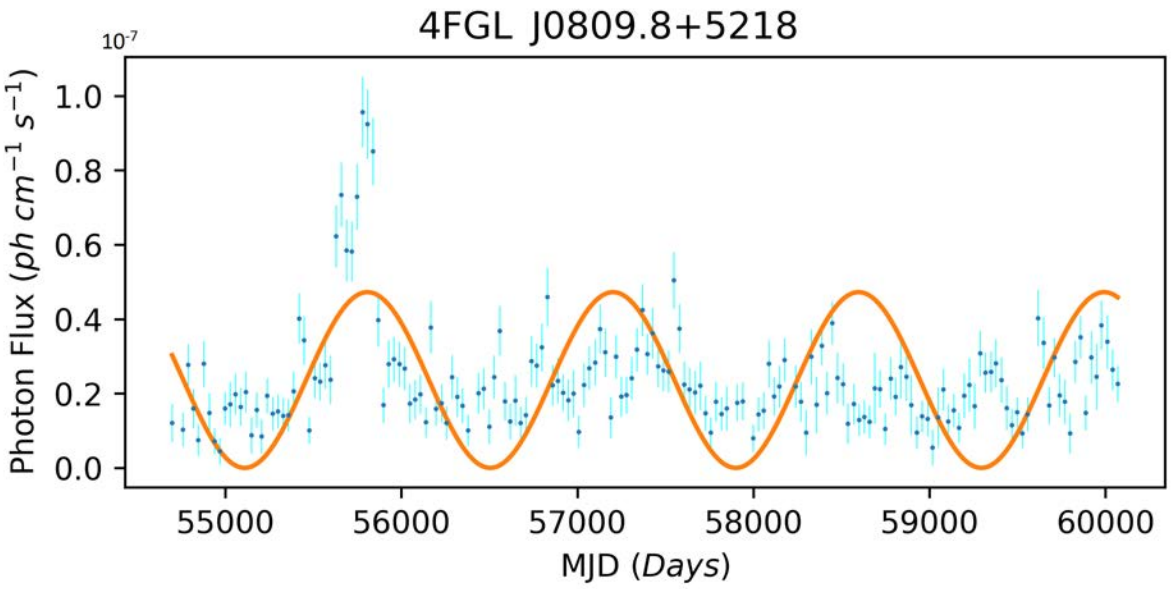

Figure 3.13: Sinusoidal curve fitted to light curve of 1ES 0806+524.

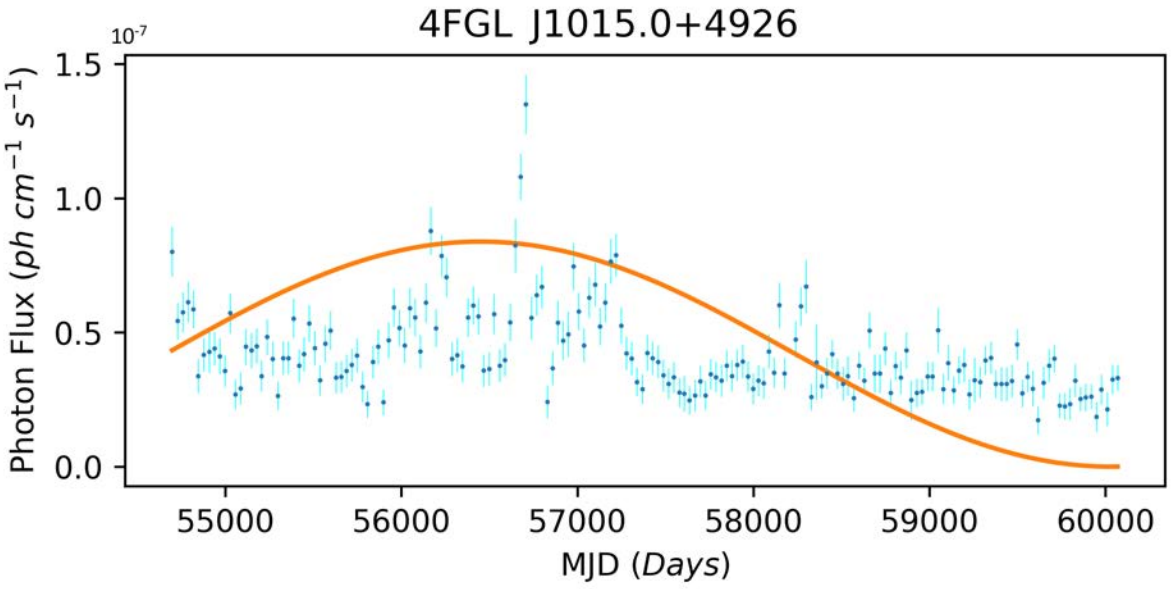

Figure 3.14: Sinusoidal curve fitted to light curve of 1H 1013+498.

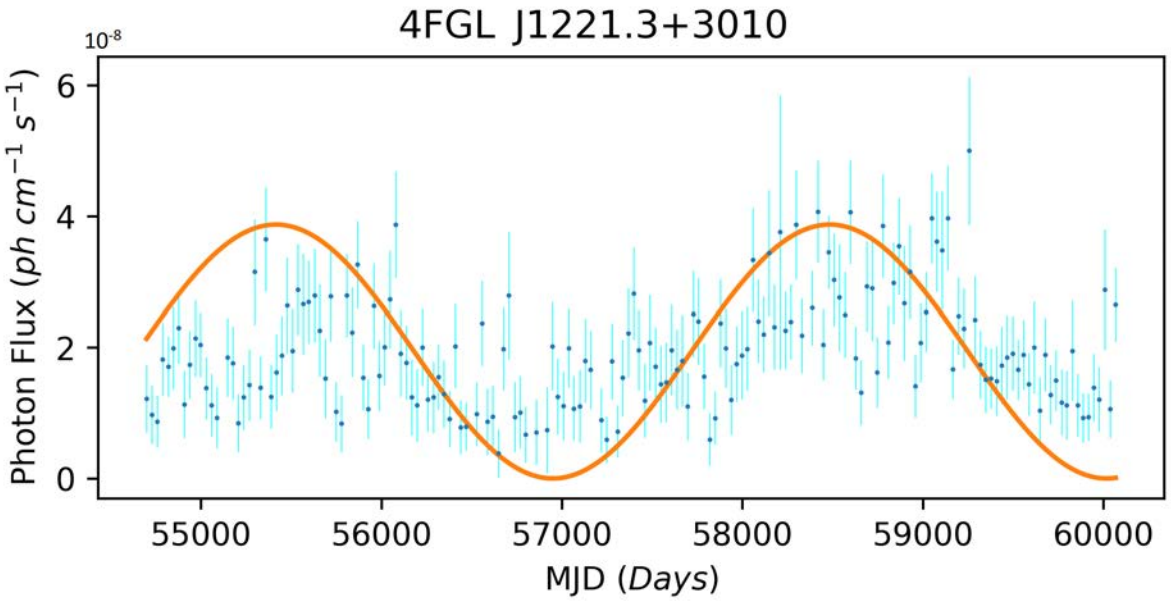

Figure 3.15: Sinusoidal curve fitted to light curve of PG 1218+304.

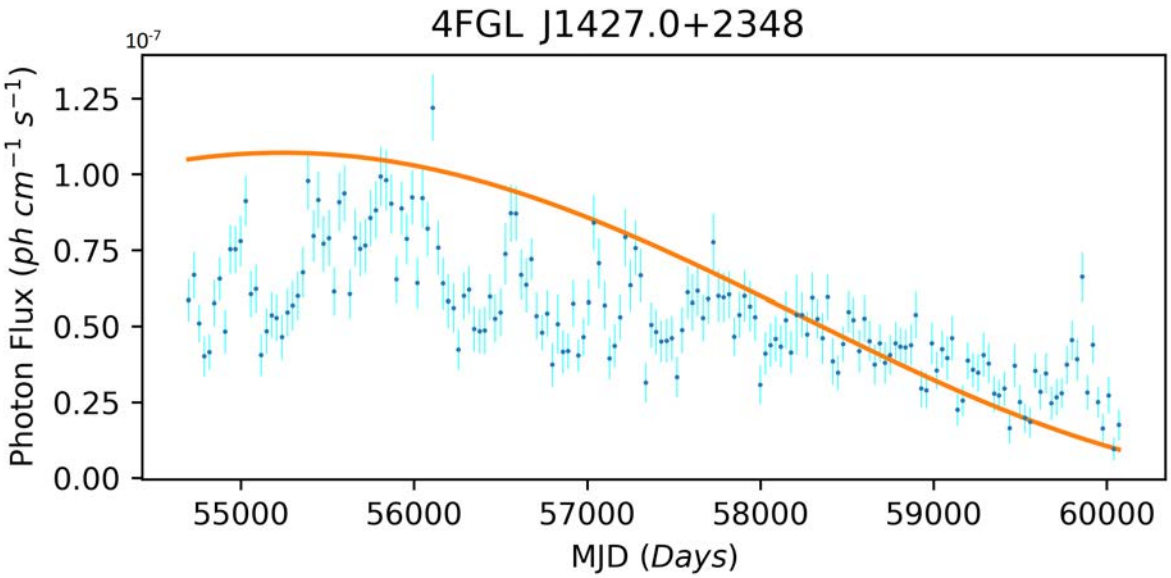

Figure 3.16: Sinusoidal curve fitted to light curve of PKS 1424+240.

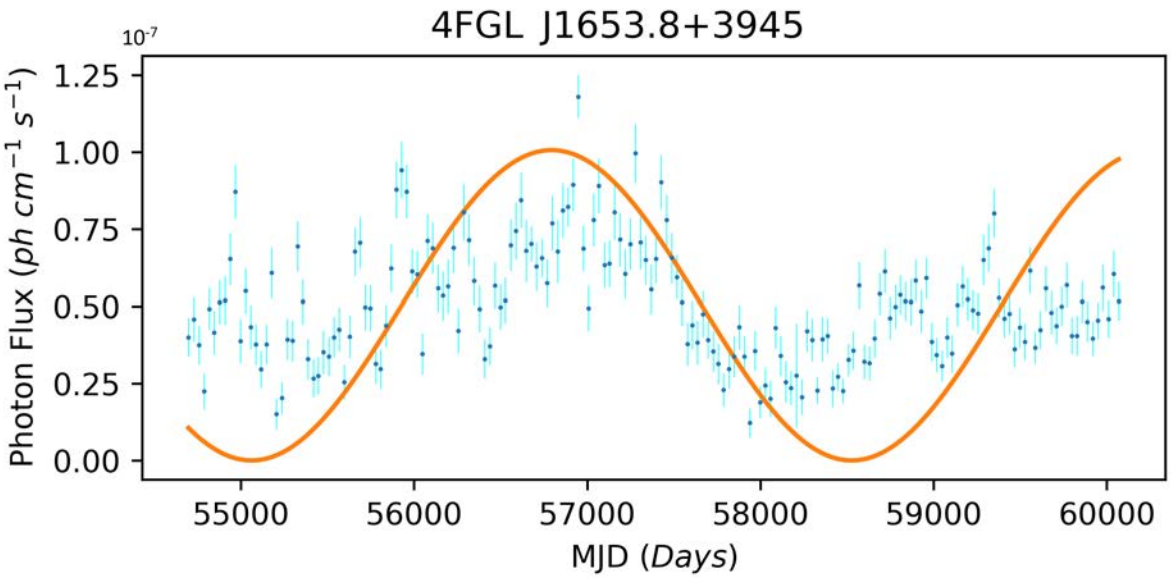

Figure 3.17: Sinusoidal curve fitted to light curve of Mkn 501.

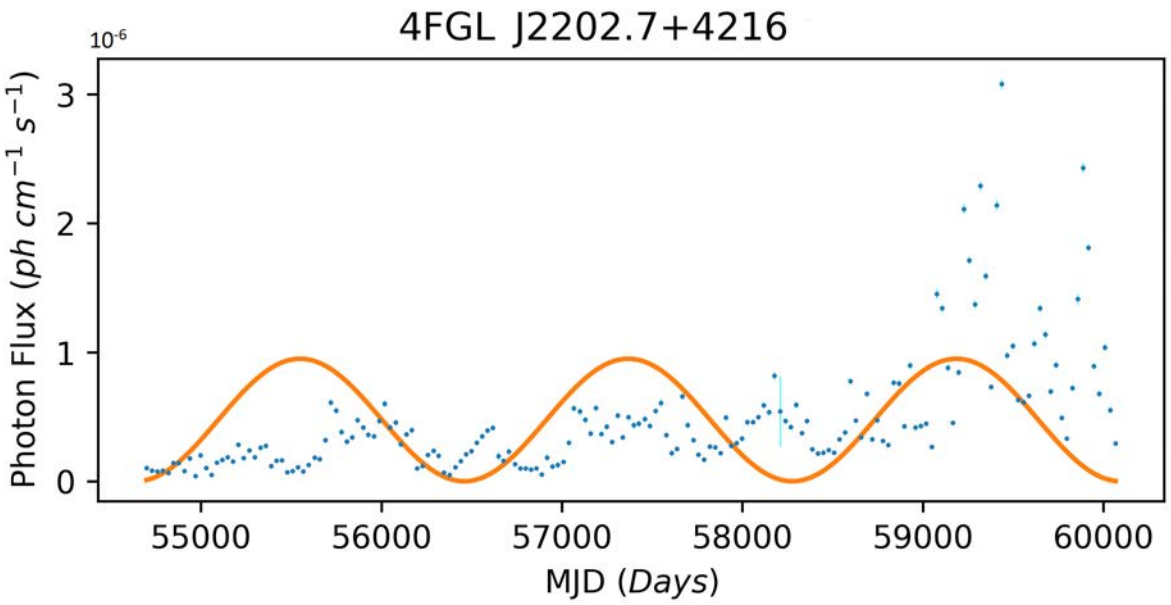

Figure 3.18: Sinusoidal curve fitted to light curve of BL Lac.

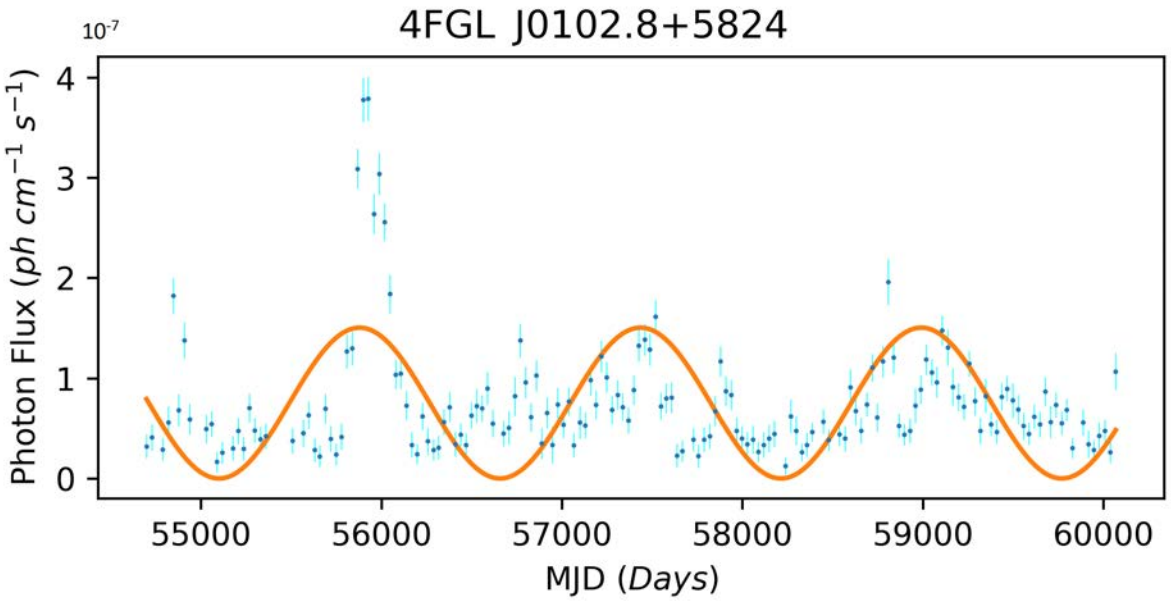

Figure 3.19: Sinusoidal curve fitted to light curve of TXS 0059+581.

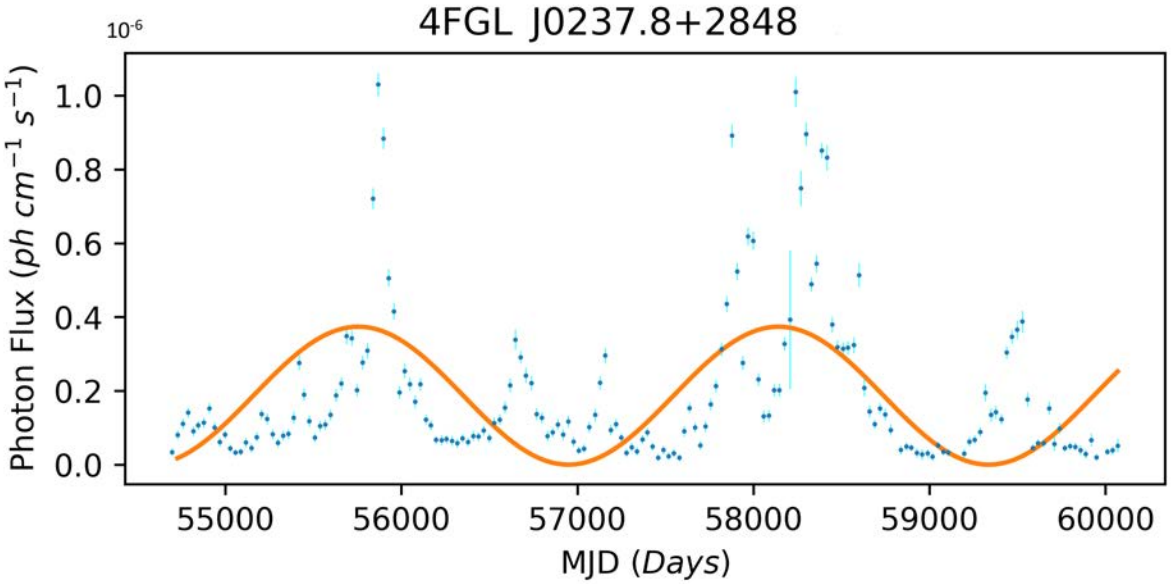

Figure 3.20: Sinusoidal curve fitted to light curve of 4C +28.07.

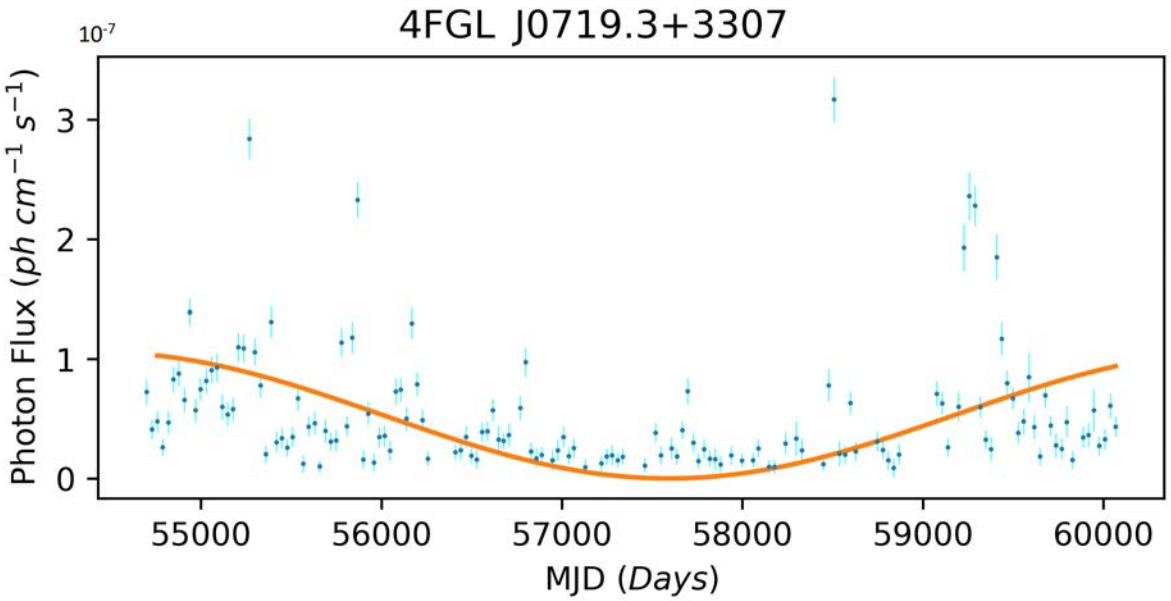

Figure 3.21: Sinusoidal curve fitted to light curve of B2 0716+33.

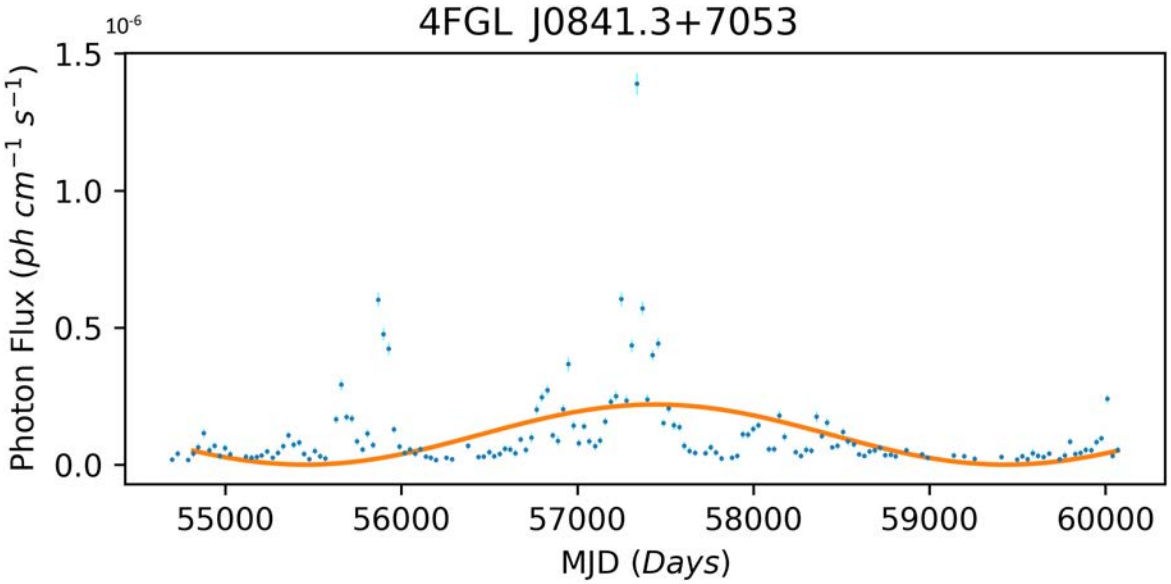

Figure 3.22: Sinusoidal curve fitted to light curve of 4C +71.07.

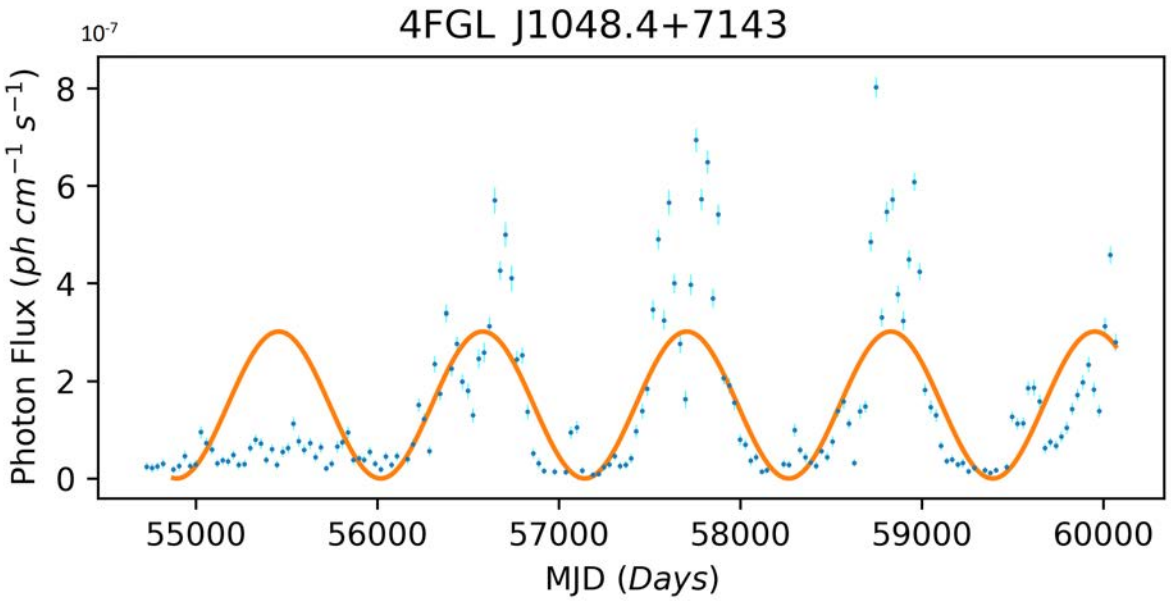

Figure 3.23: Sinusoidal curve fitted to light curve of S5 1044+71.

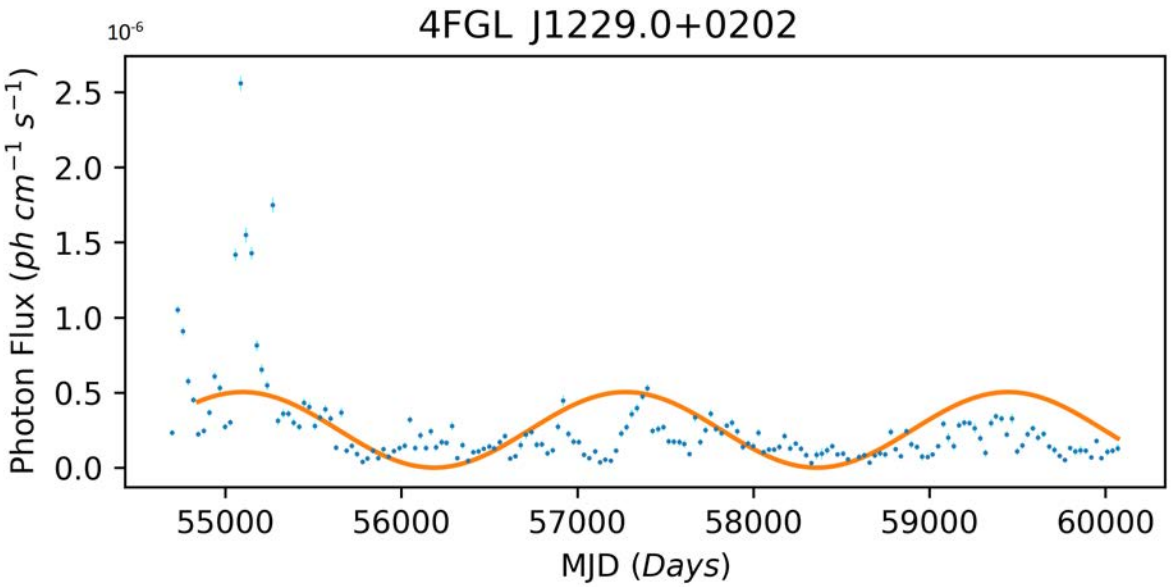

Figure 3.24: Sinusoidal curve fitted to light curve of 3C 273.

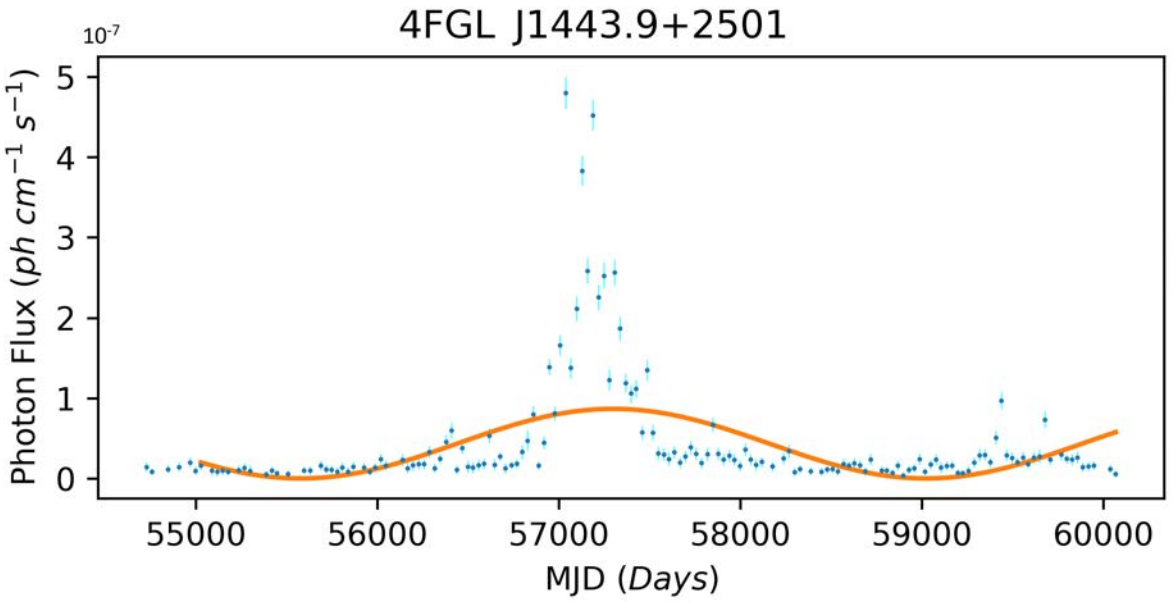

Figure 3.25: Sinusoidal curve fitted to light curve of PKS 1441+25.

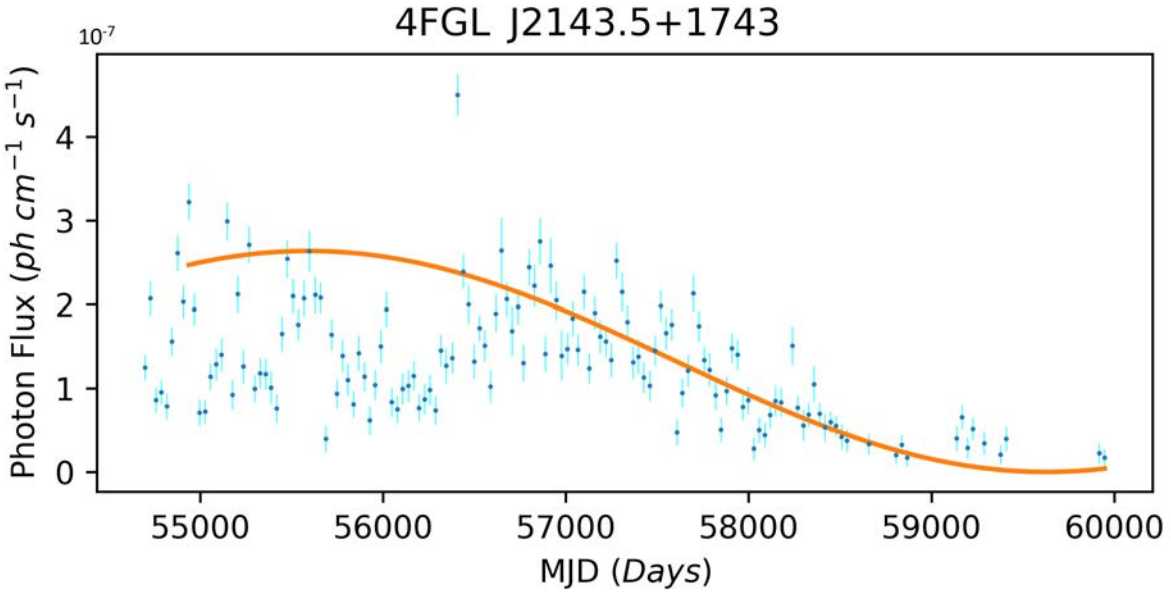

Figure 3.26: Sinusoidal curve fitted to light curve of OX 169.

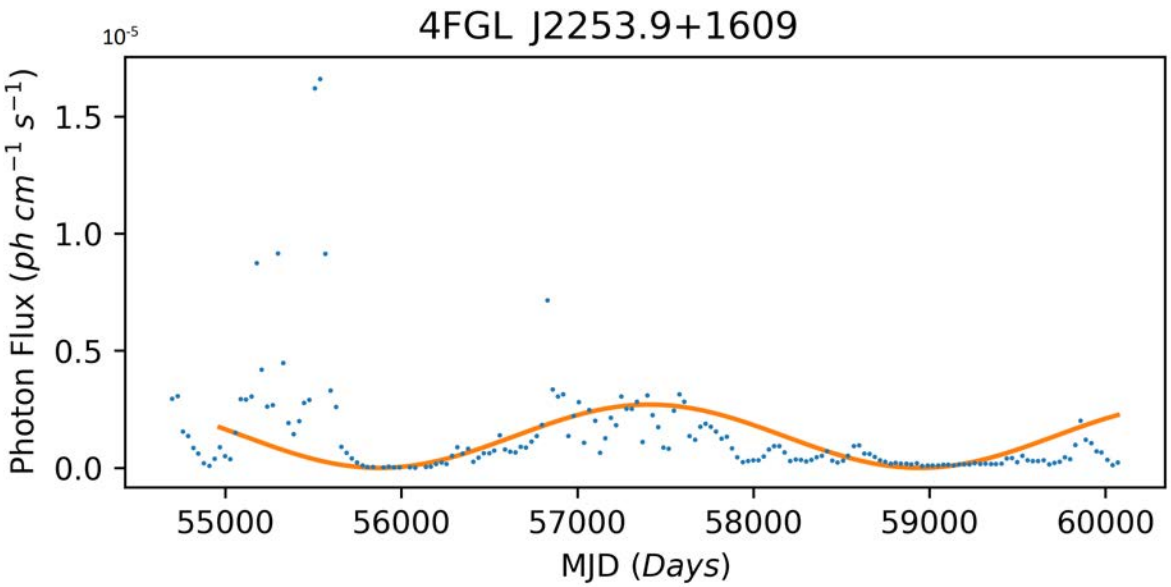

Figure 3.27: Sinusoidal curve fitted to light curve of 3C 454.3.

Further study was conducted to find a relation between found periodicities with mass and redshift. It is clearly visible from the plots that there is no correlation between periodicity with mass and redshift. It indicates that mass and age do not affect the periodicity of blazars.

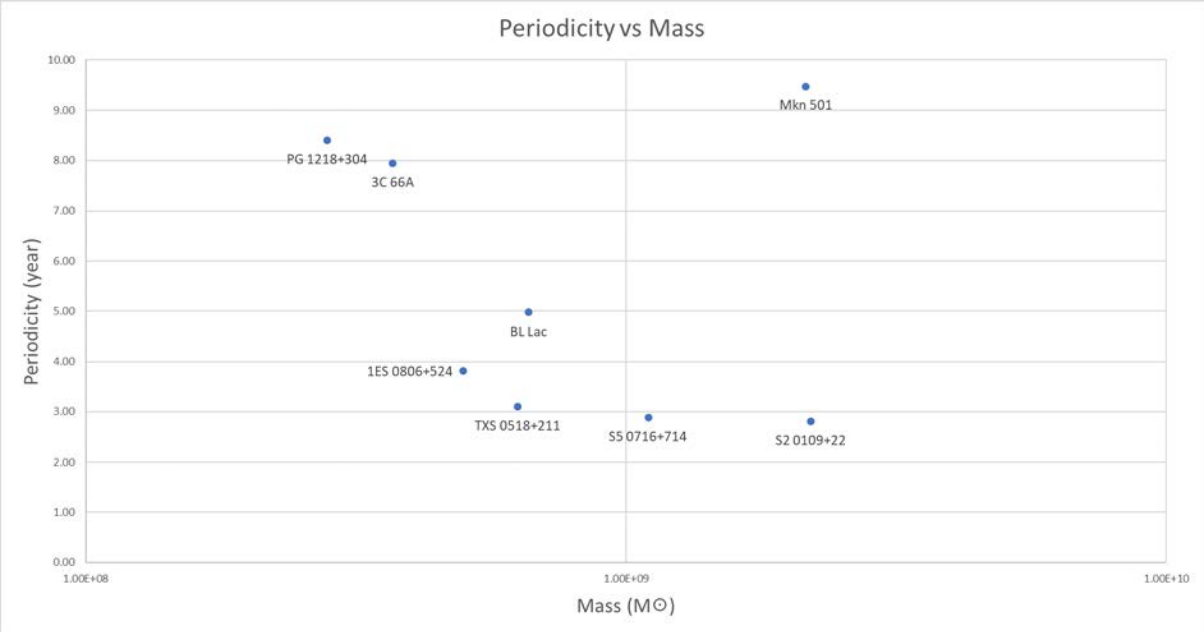

Figure 3.28: Plot of Periodicity vs Mass for BL Lac sources.

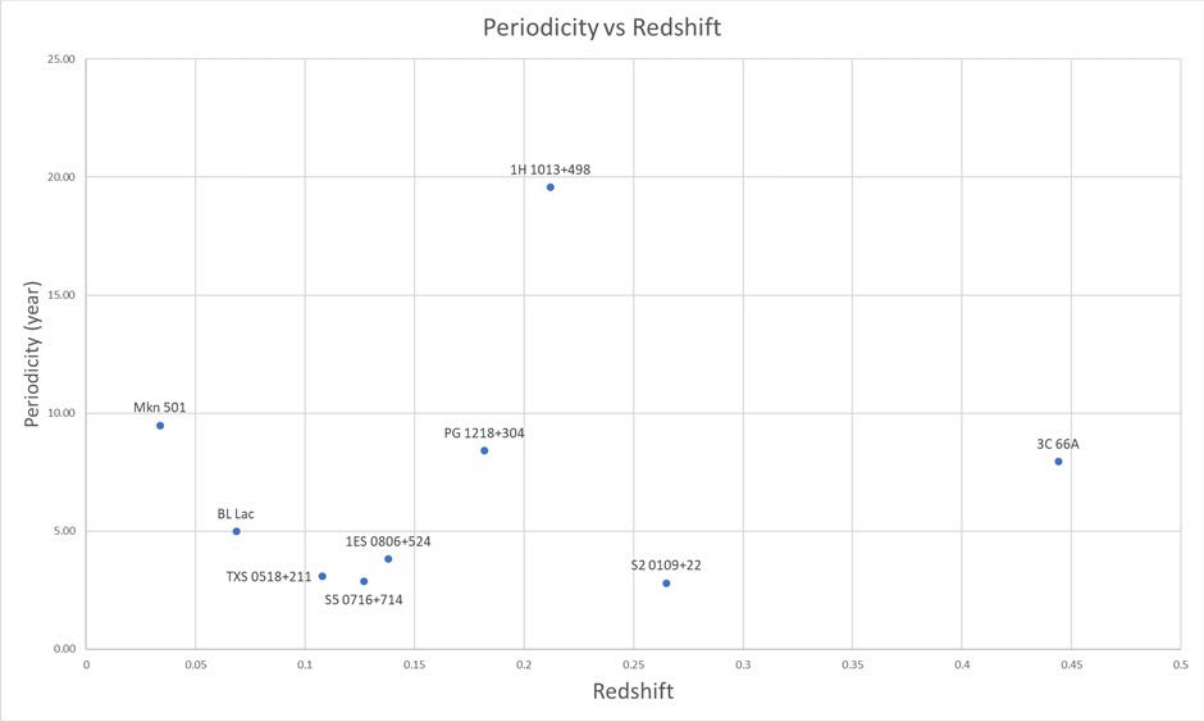

Figure 3.29: Plot of Periodicity vs Redshift for BL Lac sources.

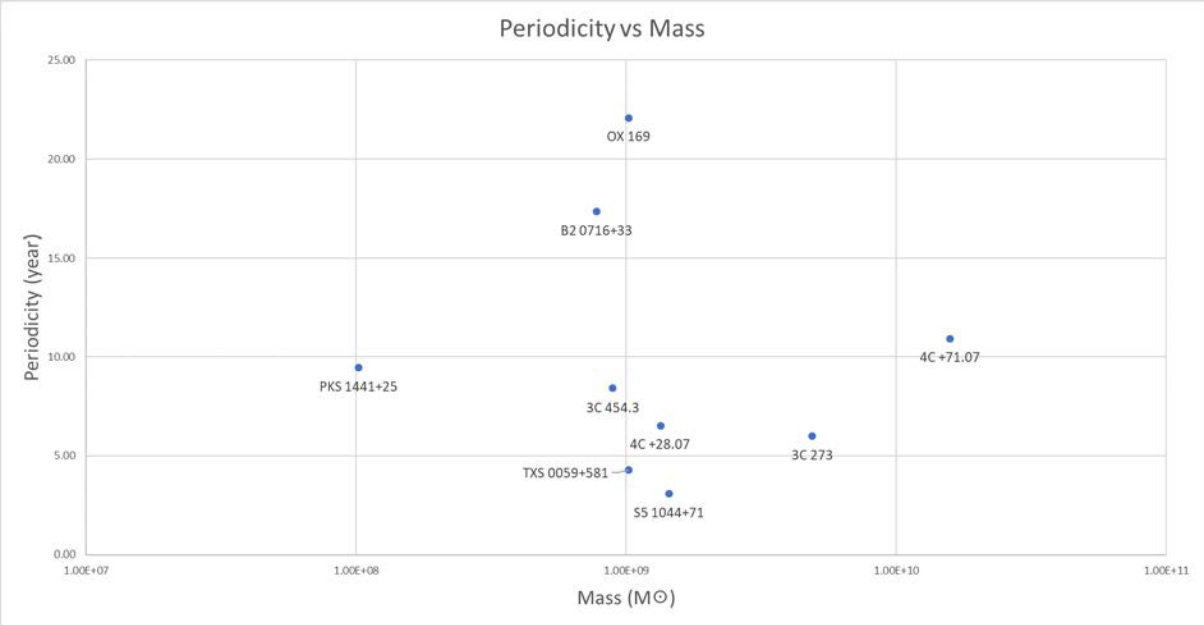

Figure 3.30: Plot of Periodicity vs Mass for FSRQ sources.

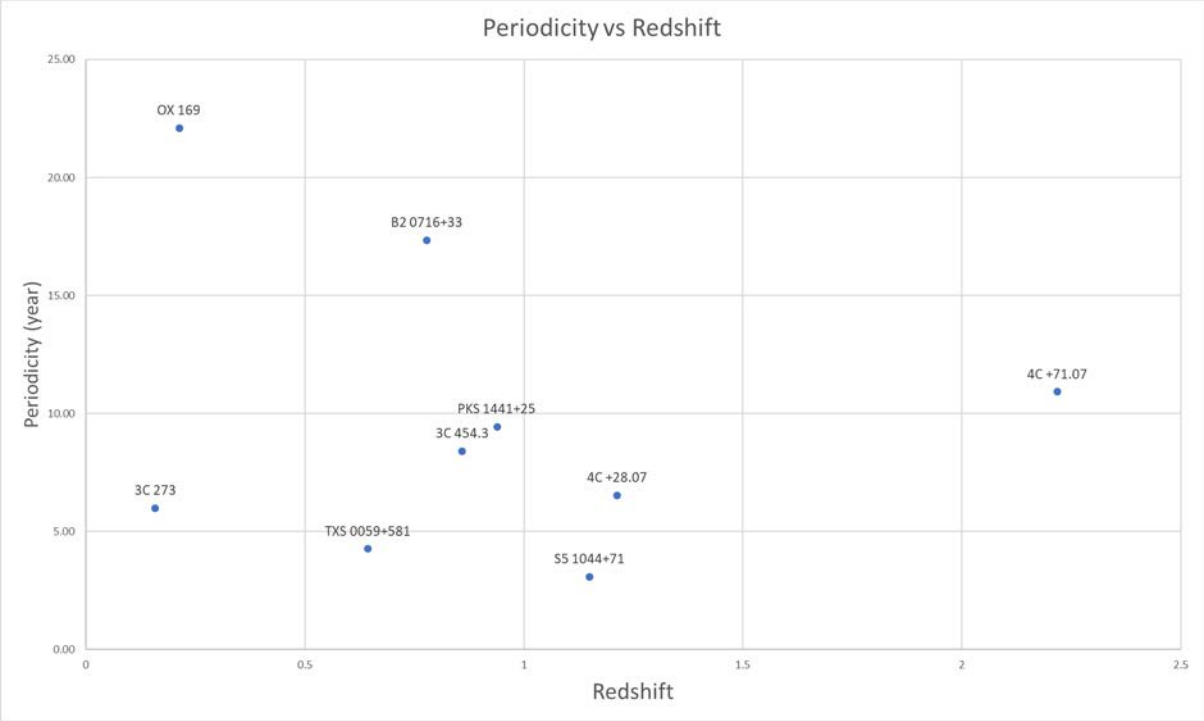

Figure 3.31: Plot of Periodicity vs Redshift for FSRQ sources.

3.2 Conclusion

From the above results, it is fair to conclude that this study has found 15 new QPOs amongst the sources, four previously found QPOs were confirmed, and one source failed to show periodicity below 95% FAP. The found frequency fit the light curves well visually for all the sources. No correlation between periodicity and mass of the AGN was found. Similarly, no correlation was found between periodicity and redshift.

3.3 Future Scope

As time passes, more long term data from various telescopes would be available for confirmation of the found QPOs. Further, multi-wavelength observations of these objects would aid in pointing to the processes behind the observed periodicities. This would open the door for multi-messenger astronomy as well, which would be a huge leap in the field.

Bibliography

[1] About Fermi-LAT Light Curve Repository. https://fermi.gsfc.nasa.gov/ssc/data/access/lat/LightCurveRepository/about.html.

[2] Fermi-LAT Instrument. https://www-glast.stanford.edu/instrument.html#:~:text=The%20LAT%20is%200.72%20m%20deep%20and%201.8,kg.%20It%20uses%20650%20W%20of%20electric%20power.

[3] Fermi-LAT Light Curve Repository. https://fermi.gsfc.nasa.gov/ssc/data/access/lat/LightCurveRepository/.

[4] Fermi-LAT: Overview. https://fermi.gsfc.nasa.gov/science/overview.html.

[5] Lomb Scargle Periodogram: Astropy. https://docs.astropy.org/en/stable/timeseries/lombscargle.html.

[6] A. Banerjee, V. Negi, R. Joshi, N. Kumar, P. J. Wiita, H. Chand, N. Rawat, X.-B. Wu, and L. C. Ho. Probable low-frequency quasi-periodic oscillations in blazars from the ztf survey. *arXiv preprint arXiv:2210.07266*, 2022.

[7] J. M. Bardeen and J. A. Petterson. The lense-thirring effect and accretion disks around kerr black holes. *Astrophysical Journal Letters v. 195, p. L65*, 195:L65, 1975.

[8] S. Chandra, K. Baliyan, S. Ganesh, and U. Joshi. Rapid optical variability in blazar s5 0716+ 71 during 2010 march. *The Astrophysical Journal*, 731(2):118, 2011.

[9] Y. Gong, T. Yi, X. Yang, H. Li, X. Chang, J. Chen, and Z. Chen. Multi-wavelength search for quasi-periodic oscillations in bl lac 4fgl j0112. 1+ 2245. *Astrophysics and Space Science*, 367(1):6, 2022.

[10] M. J. Graham, S. Djorgovski, D. Stern, A. J. Drake, A. A. Mahabal, C. Donalek, E. Glikman, S. Larson, and E. Christensen. A systematic search for close supermassive black hole binaries in the catalina real-time transient survey. *Monthly Notices of the Royal Astronomical Society*, 453(2):1562–1576, 2015.

[11] A. Grossmann and J. Morlet. Decomposition of hardy functions into square integrable wavelets of constant shape. *SIAM journal on mathematical analysis*, 15(4):723–736, 1984.

[12] N. Kaur, K. S. Baliyan, and S. Ganesh. Optical intra-day variability in 3c 66a: A decade of observations. *Monthly Notices of the Royal Astronomical Society*, 469(2):2305–2312, 2017.

[13] D. i. Kranich, O. De Jager, M. Kestel, E. Lorenz, et al. Evidence for a qpo structure in the tev and x-ray light curve during the 1997 high state gamma emission of mkn 501. *arXiv preprint astro-ph/9907205*, 1999.

[14] X.-P. Li, H.-Y. Yang, Y. Cai, A. Lähteenmäki, M. Tornikoski, J. Tammi, S. Suutarinen, H.-T. Yang, Y.-H. Luo, and L.-S. Wang. Radio and γ-ray variability in blazar s5 0716+ 714: A year-like quasi-periodic oscillation in the radio light curve. *The Astrophysical Journal*, 943(2):157, 2023.

[15] N. R. Lomb. Least-squares frequency analysis of unequally spaced data. *Astrophysics and space science*, 39:447–462, 1976.

[16] J.-F. Lu and B.-Y. Zhou. Observational evidence of jet precession in galactic nuclei caused by accretion disks. *The Astrophysical Journal*, 635(1):L17, 2005.

[17] Z. Osmanov. Is very high energy emission from the bl lac 1es 0806+ 524 centrifugally driven? *New Astronomy*, 15(4):351–355, 2010.

[18] D. Osterbrock. Active galactic nuclei. *Reports on Progress in Physics*, 54(4):579, 1991.

[19] P. Padovani, D. Alexander, R. Assef, B. De Marco, P. Giommi, R. Hickox, G. Richards, V. Smolčić, E. Hatziminaoglou, V. Mainieri, et al. Active galactic nuclei: what's in a name? *The Astronomy and Astrophysics Review*, 25:1–91, 2017.

[20] V. S. Paliya, A. Domínguez, M. Ajello, A. Olmo-García, and D. Hartmann. The central engines of fermi blazars. *The Astrophysical Journal Supplement Series*, 253(2):46, 2021.

[21] C. M. Raiteri, M. Villata, J. Acosta-Pulido, I. Agudo, A. Arkharov, R. Bachev, G. Baida, E. Benítez, G. Borman, W. Boschin, et al. Blazar spectral variability as explained by a twisted inhomogeneous jet. *Nature*, 552(7685):374–377, 2017.

[22] J. D. Scargle. Studies in astronomical time series analysis. ii-statistical aspects of spectral analysis of unevenly spaced data. *Astrophysical Journal, Part 1, vol. 263, Dec. 15, 1982, p. 835-853.*, 263:835–853, 1982.

[23] M. S. Shaw, R. W. Romani, G. Cotter, S. E. Healey, P. F. Michelson, A. C. Readhead, J. L. Richards, W. Max-Moerbeck, O. G. King, and W. J. Potter. Spectroscopy of the largest ever γ-ray-selected bl lac sample. *The Astrophysical Journal*, 764(2):135, 2013.

[24] A. Sillanpaa, S. Haarala, M. Valtonen, B. Sundelius, and G. Byrd. Oj 287-binary pair of supermassive black holes. *Astrophysical Journal, Part 1 (ISSN 0004-637X), vol. 325, Feb. 15, 1988, p. 628-634. Research supported by Nordisk Institut for Teoretisk Atomfysik and NSF.*, 325:628–634, 1988.

[25] K. K. Singh and P. J. Meintjes. Characterization of variability in blazar light curves. *Astronomische Nachrichten*, 341(6-7):713–725, 2020.

[26] A. Stockton and T. Farnham. Ox 169-evidence for a recent merger. *Astrophysical Journal, Part 1 (ISSN 0004-637X), vol. 371, April 20, 1991, p. 525-534.*, 371:525–534, 1991.

[27] S.-S. Sun, H.-L. Li, X. Yang, J. Lü, D.-W. Xu, and J. Wang. The intra-day optical monitoring of bl lacerate object 1es 1218+ 304 at its highest x-ray flux level. *Research in Astronomy and Astrophysics*, 21(8):197, 2021.

[28] M. Templeton. Time-series analysis of variable star data. *The Journal of the American Association of Variable Star Observers, vol. 32, no. 1, p. 41-54*, 32:41–54, 2004.

[29] A. Ulubay-Siddiki, O. Gerhard, and M. Arnaboldi. Self-gravitating warped discs around supermassive black holes. *Monthly Notices of the Royal Astronomical Society*, 398(2):535–547, 2009.

[30] J. T. VanderPlas. Understanding the lomb–scargle periodogram. *The Astrophysical Journal Supplement Series*, 236(1):16, 2018.

[31] G. Wang, J. Cai, and J. Fan. A possible 3 yr quasi-periodic oscillation in γ-ray emission from the fsrq s5 1044+ 71. *The Astrophysical Journal*, 929(2):130, 2022.

[32] P.-f. Zhang, D.-h. Yan, J.-n. Zhou, J.-c. Wang, and L. Zhang. Searching for quasiperiodic modulations in γ-ray active galactic nuclei. *The Astrophysical Journal*, 891(2):163, 2020.

Turnitin Originality Report

Processed on: 31-Jul-2023 05:25 IST

ID: 2139073153

Word Count: 4652

Submitted: 1

Master Thesis By Pranjal Chaturvedi

Similarity Index

11%

Similarity by Source

Internet Sources:	7%
Publications:	8%
Student Papers:	2%

2% match (C. M. Raiteri, M. Villata, J. A. Acosta-Pulido, I. Agudo et al. "Blazar spectral variability as explained by a twisted inhomogeneous jet", Nature, 2017)
C. M. Raiteri, M. Villata, J. A. Acosta-Pulido, I. Agudo et al. "Blazar spectral variability as explained by a twisted inhomogeneous jet", Nature, 2017

1% match (Junping Chen, Tingfeng Yi, Yunlu Gong, Xing Yang, Zhihui Chen, Xin Chang, Lisheng Mao. "A 31.3 day Transient Quasiperiodic Oscillation in Gamma-ray Emission from Blazar S5 0716+714", The Astrophysical Journal, 2022)
Junping Chen, Tingfeng Yi, Yunlu Gong, Xing Yang, Zhihui Chen, Xin Chang, Lisheng Mao. "A 31.3 day Transient Quasiperiodic Oscillation in Gamma-ray Emission from Blazar S5 0716+714", The Astrophysical Journal, 2022

1% match ()
Graham, Matthew J., Djorgovski, S. G. et al. "A systematic search for close supermassive black hole binaries in the Catalina Real-time Transient Survey", Royal Astronomical Society, 2015

1% match (Abhradeep Roy, Arkadipta Sarkar, Anshu Chatterjee, Alok C Gupta, Varsha Chitnis, P J Wiita. "Transient quasi-periodic oscillations at γ-rays in the TeV blazar PKS 1510-089", Monthly Notices of the Royal Astronomical Society, 2022)
Abhradeep Roy, Arkadipta Sarkar, Anshu Chatterjee, Alok C Gupta, Varsha Chitnis, P J Wiita. "Transient quasi-periodic oscillations at γ-rays in the TeV blazar PKS 1510-089", Monthly Notices of the Royal Astronomical Society, 2022

1% match (student papers from 30-May-2023)
Submitted to University of Malaya on 2023-05-30

1% match (Internet from 23-Feb-2023)
https://www.science.gov/topicpages/r/ray+flaring+blazar

< 1% match (Graham, Matthew J., S. G. Djorgovski, Daniel Stern, Andrew J. Drake, Ashish A. Mahabal, Ciro Donalek, Eilat Glikman, Steve Larson, and Eric Christensen. "A systematic search for close supermassive black hole binaries in the Catalina Real-time Transient Survey", Monthly Notices of the Royal Astronomical Society, 2015.)
Graham, Matthew J., S. G. Djorgovski, Daniel Stern, Andrew J. Drake, Ashish A. Mahabal, Ciro Donalek, Eilat Glikman, Steve Larson, and Eric Christensen. "A systematic search for close supermassive black hole binaries in the Catalina Real-time Transient Survey", Monthly Notices of the Royal Astronomical Society, 2015.

< 1% match (Gustavo Rodrigues Romano Soares. "Accretion discs, jets, and black hole spins: a study of blazars", Universidade de Sao Paulo, Agencia USP de Gestao da Informacao Academica (AGUIA), 2020)
Gustavo Rodrigues Romano Soares. "Accretion discs, jets, and black hole spins: a